11.05.2023
PHENIICS FEST
In-beam gamma-ray spectroscopy of the exotic 79Cu

Massyl KACI

2022/2023

Outline:

1. Introduction

1.1. Scientific context
1.2. Current state of knowledge

2. Data analysis

2.1. Particle Identification of the beam nuclei
2.2. Energy calibration of HiCARI Ge array
2.3. Velocity determination
2.3. Preliminary Doppler-corrected gamma-spectra

3. Conclusion and outlook

1. Introduction
1.1. Scientific context

<u>In nuclear physics:</u>

- Diversity and complexity of the phenomena.
- No unified theory but only specific models.

Phenomenon	Model/Theory
α-decay	Gamow theory
β-decay	Fermi gas model
Fission	Liquid drop model
γ-deexcitation	**Nuclear shell model**

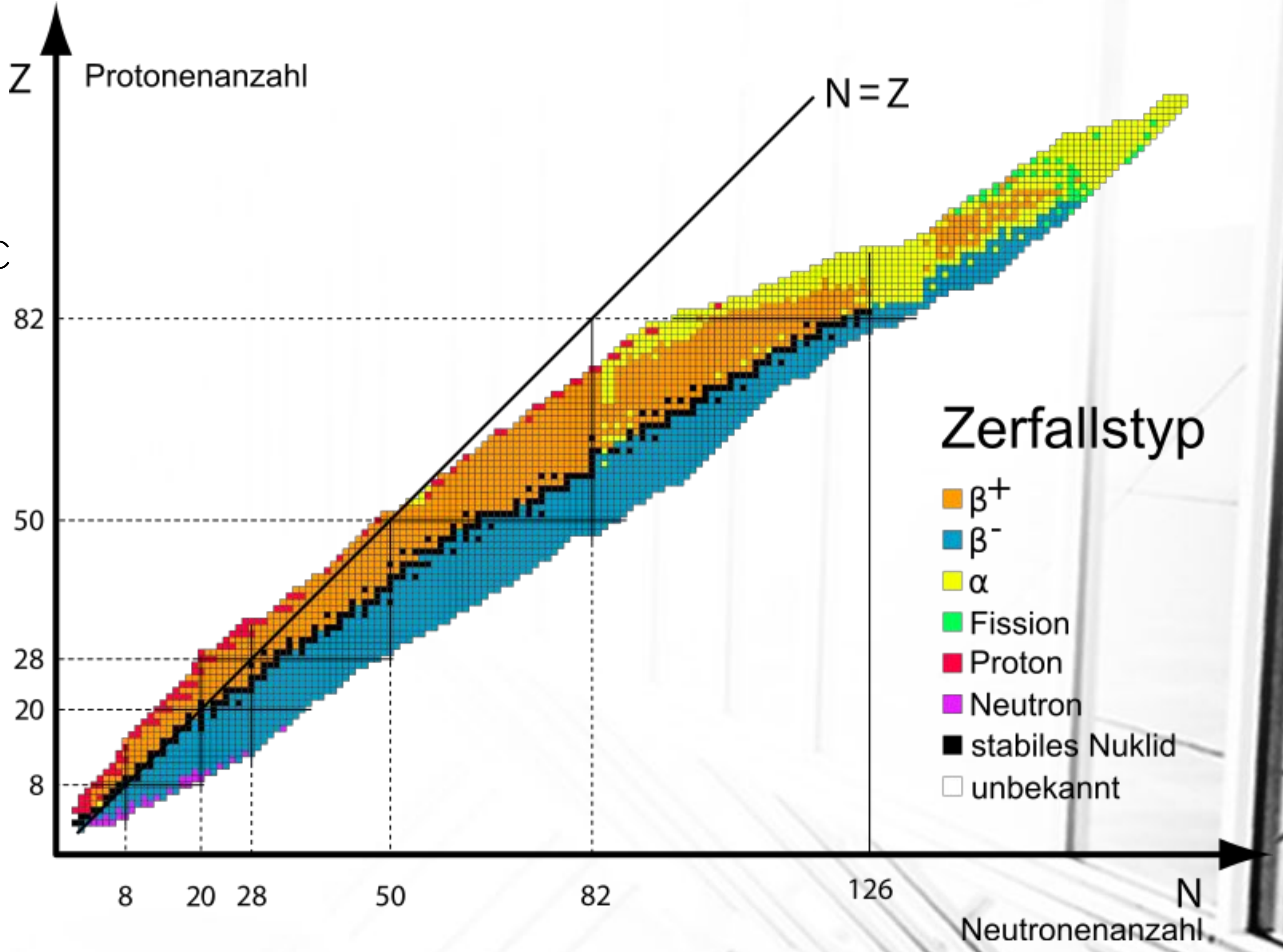

1. Introduction
1.1. Scientific context

Shell model and ɣ radioactivity:

- The shell model was motivated by the observation of extra stability for isotopes with a special number of N and/or Z (magic numbers) like inert gases in atomic physics.

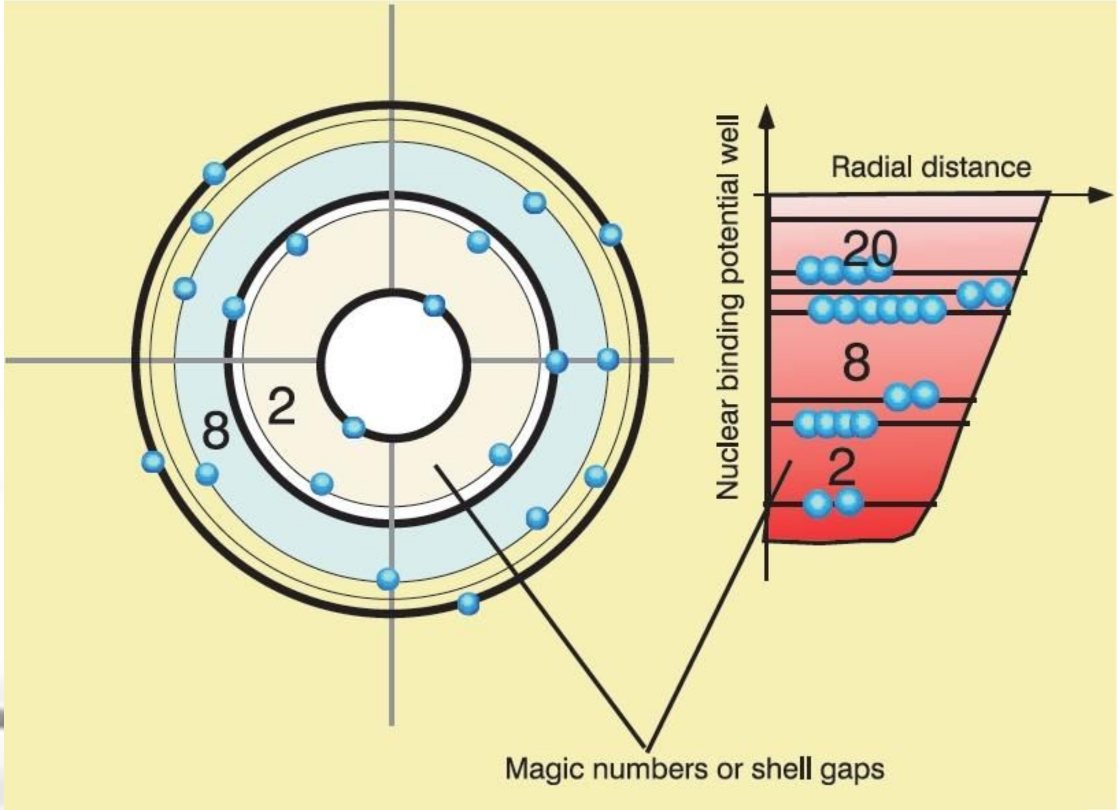

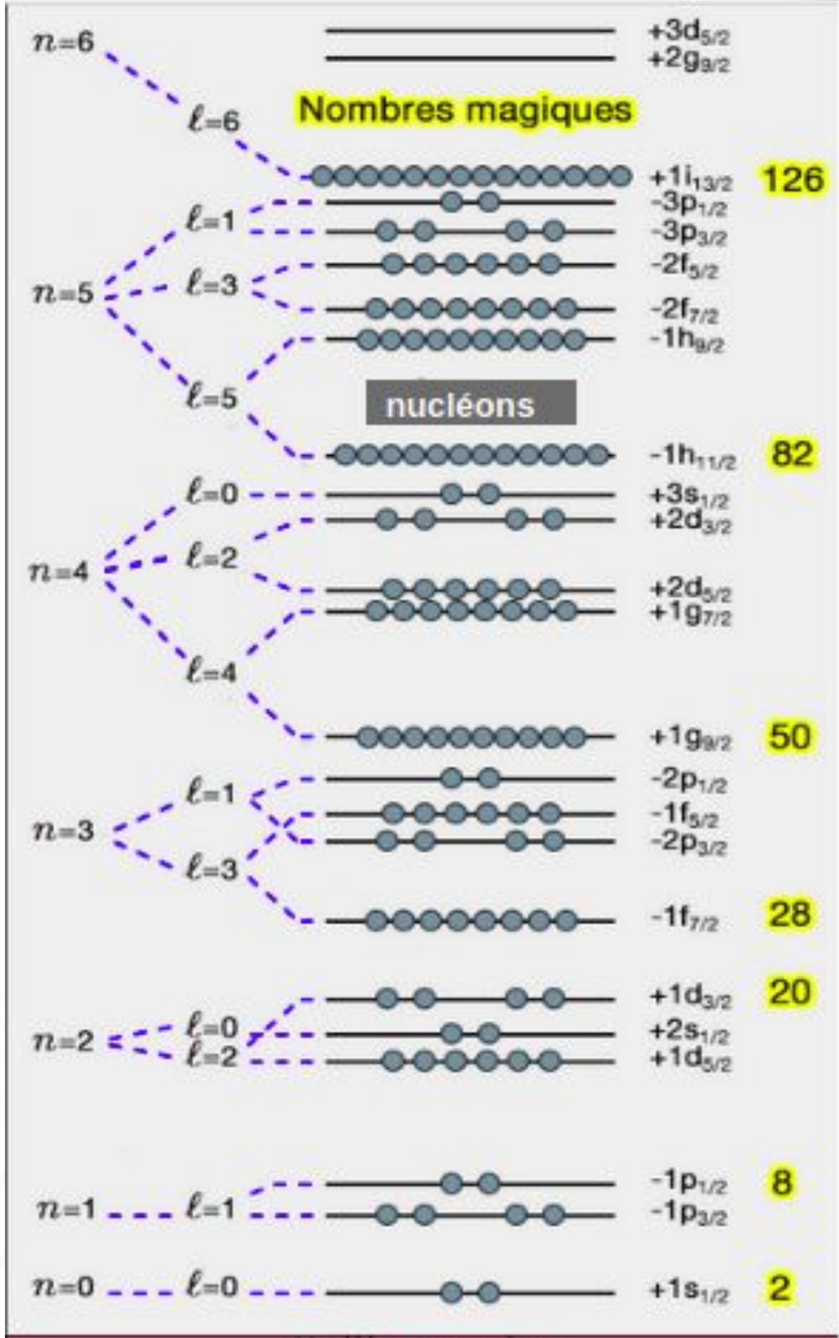

Modèle en couches
(Figure : vetopsy.fr)

1. Introduction
1.1. Scientific context

Shell model and ɣ radioactivity:

- The shell model was motivated by the observation of extra stability for isotopes with a magic number of N and/or Z.
- ɣ radioactivity: Deexcitation of a nucleus due to the transition of a nucleon from a higher to a lower energy state.

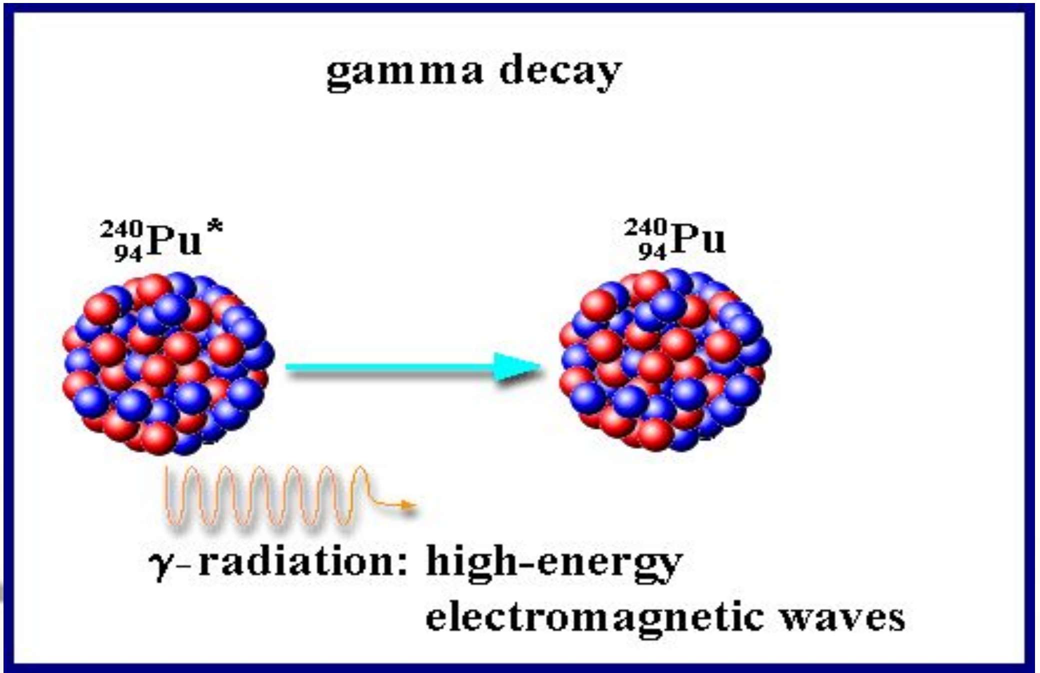

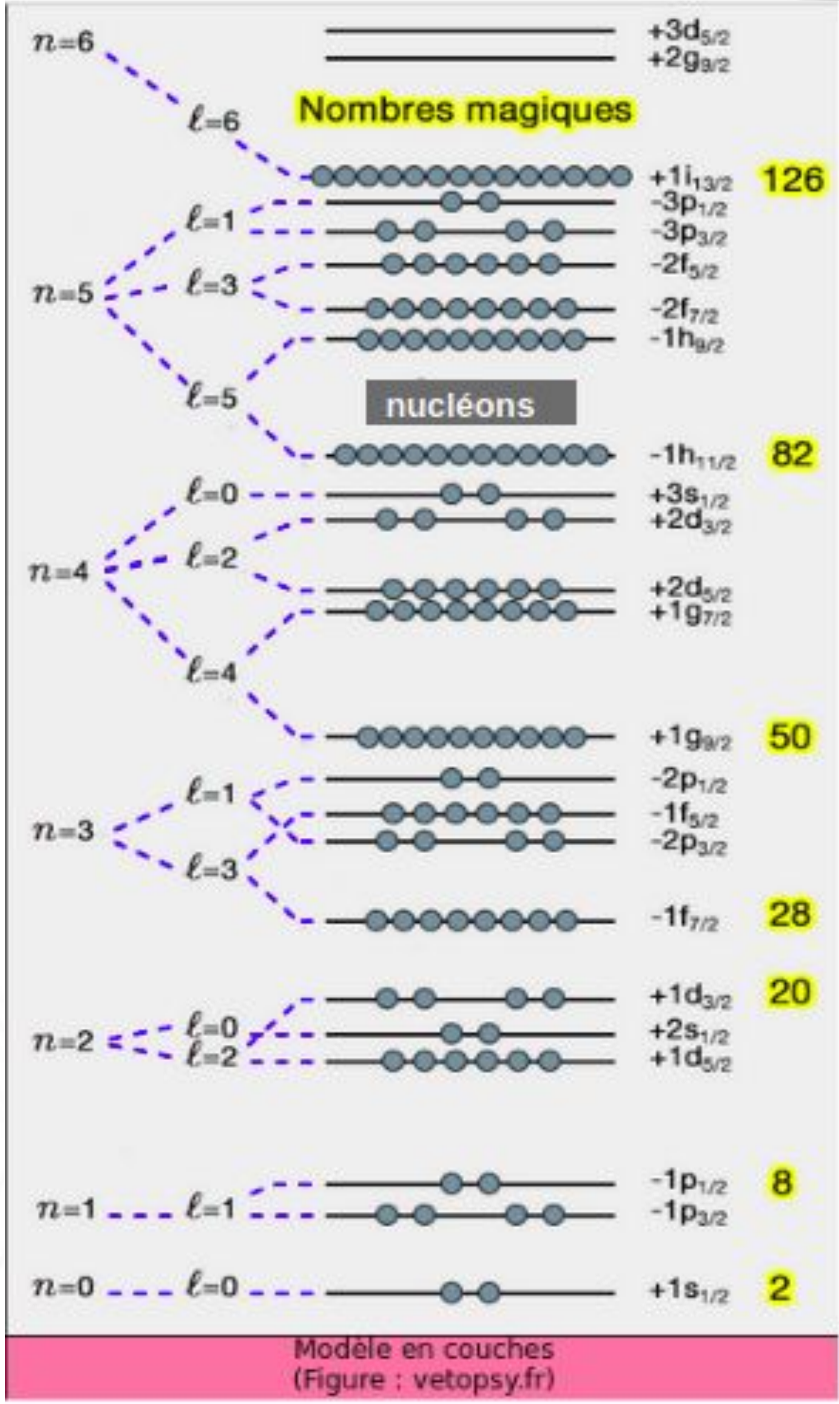

1. Introduction
1.1. Scientific context

Shell model and ɣ radioactivity:

Challenges:

- Evolution of shell gaps and magic numbers (far from the stability valley).
- Possibility of inverting the order of the states (depending on Z and N).

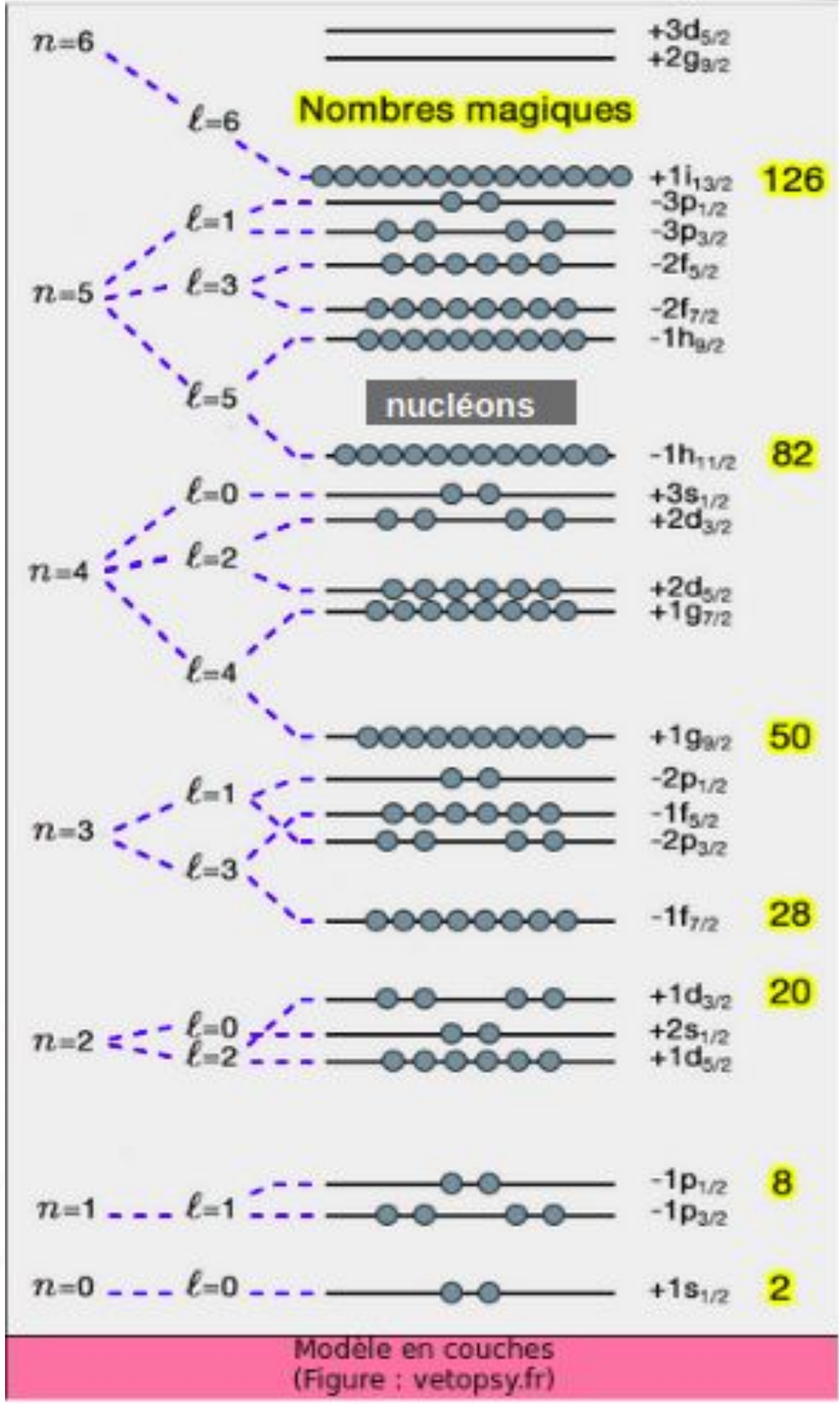

1. Introduction
1.1. Scientific context

Shell model and ɣ radioactivity:

Challenges:

- Evolution of shell gaps and magic numbers (far from the stability valley).
- Possibility of inverting the order of the states (depending on Z and N).

→ Necessary to study exotic nuclei having a large N/Z asymmetry.

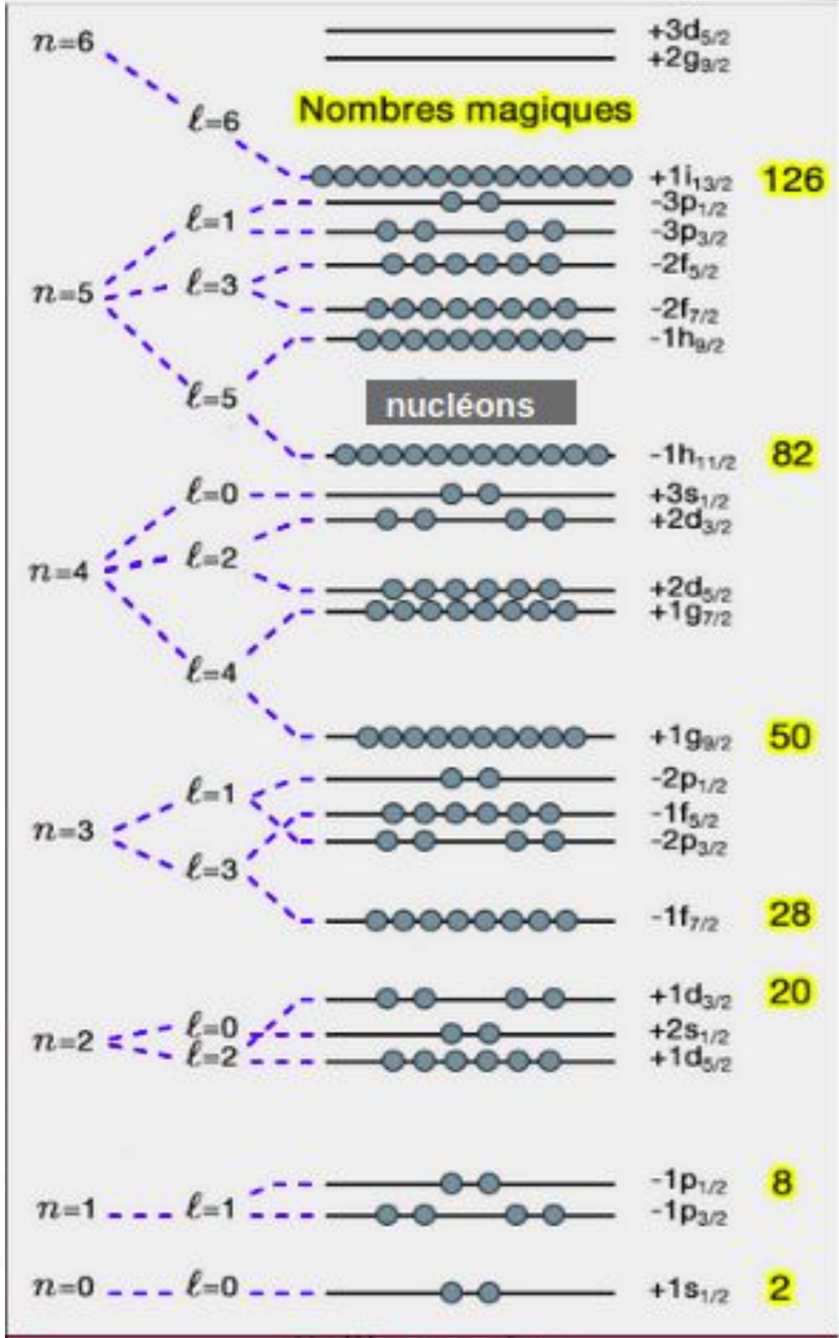

Modèle en couches
(Figure : vetopsy.fr)

1. Introduction
1.1. Scientific context

Shell model and ɣ radioactivity:

Challenges:

- Evolution of shell gaps and magic numbers (far from the stability valley).
- Possibility of inverting the order of the states (depending on Z and N).

→ Necessary to study exotic nuclei having a large N/Z asymmetry.

→ Candidate: ^{78}Ni (Z=28, N=50)

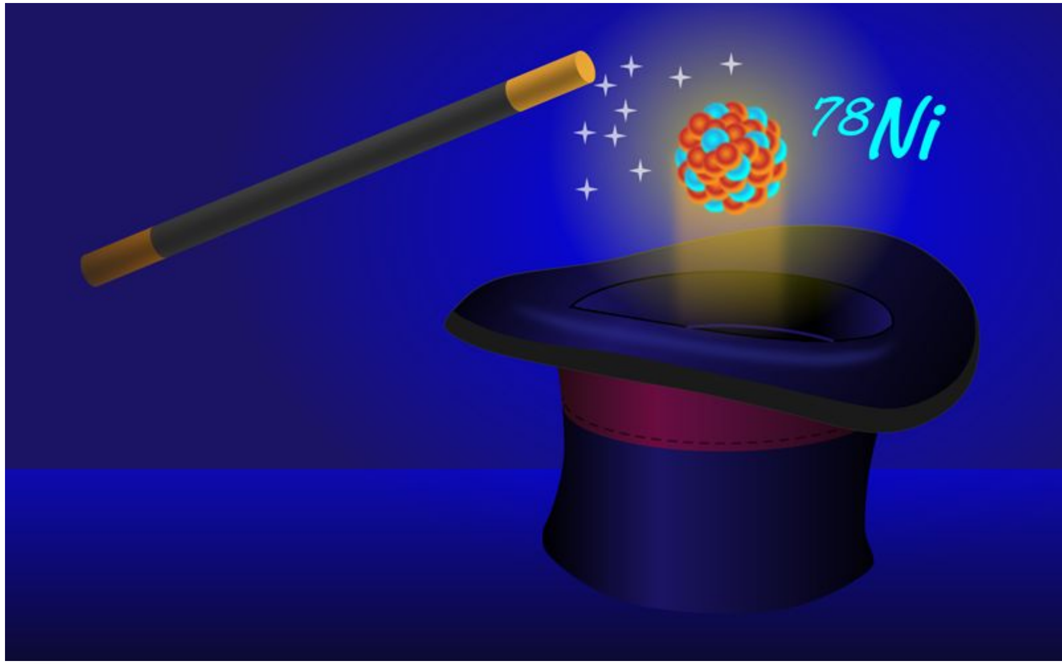

1. Introduction
1.1. Scientific context

Shell model and ɣ radioactivity:

Challenges:
- Evolution of shell gaps and magic numbers (far from the stability valley).
- Possibility of inverting the order of the states (depending on Z and N).

⟶ Necessary to study exotic nuclei having a large N/Z asymmetry.

⟶ Candidate: ^{78}Ni (Z=28, N=50) through the study of ^{79}Cu

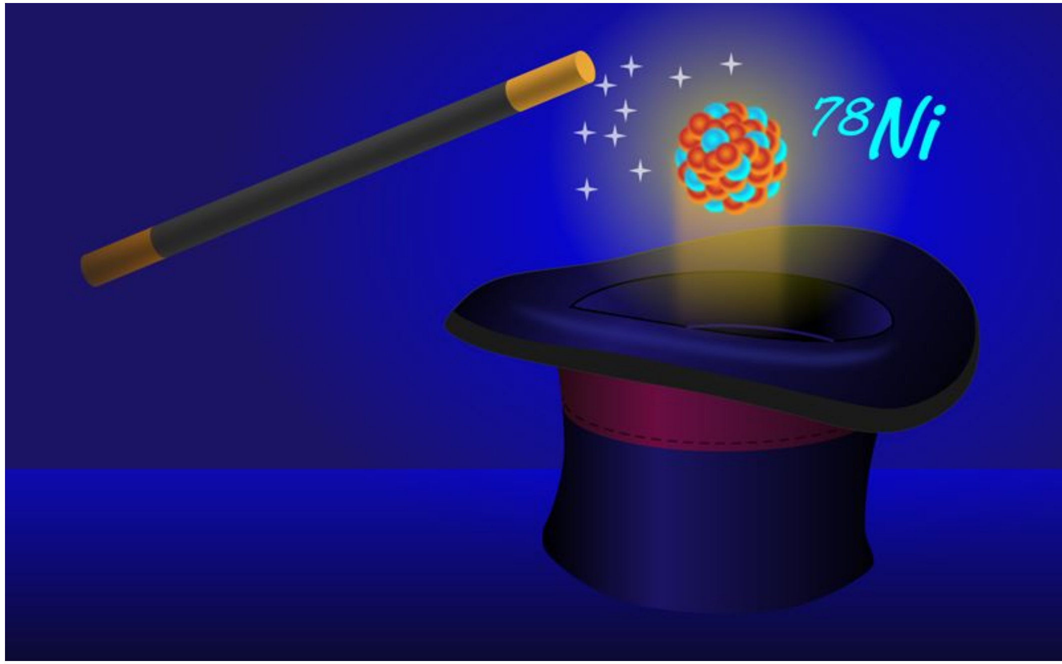

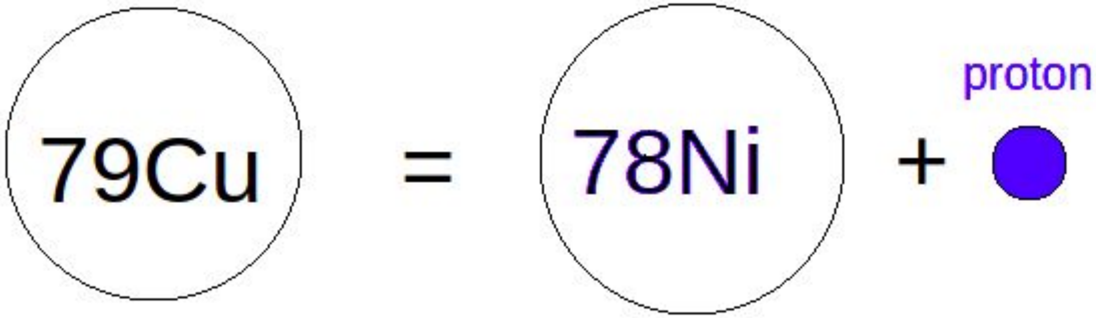

1. Introduction

1.2. Current state of knowledge

<u>First spectroscopy of 79Cu (2014 SEASTAR campaign at RIKEN):</u>

- Beam of 238U (at β ~ 0.6) .
- Induced in-flight fission at a primary 9Be production target (F0).
- Selection of 80Zn isotopes (BigRIPS).
- Collision on a secondary target (liquid hydrogen) at F8 and knock-out of a proton

→ 80Zn(p,2p)79Cu

- Detection of the emitted γ-rays using scintillators.

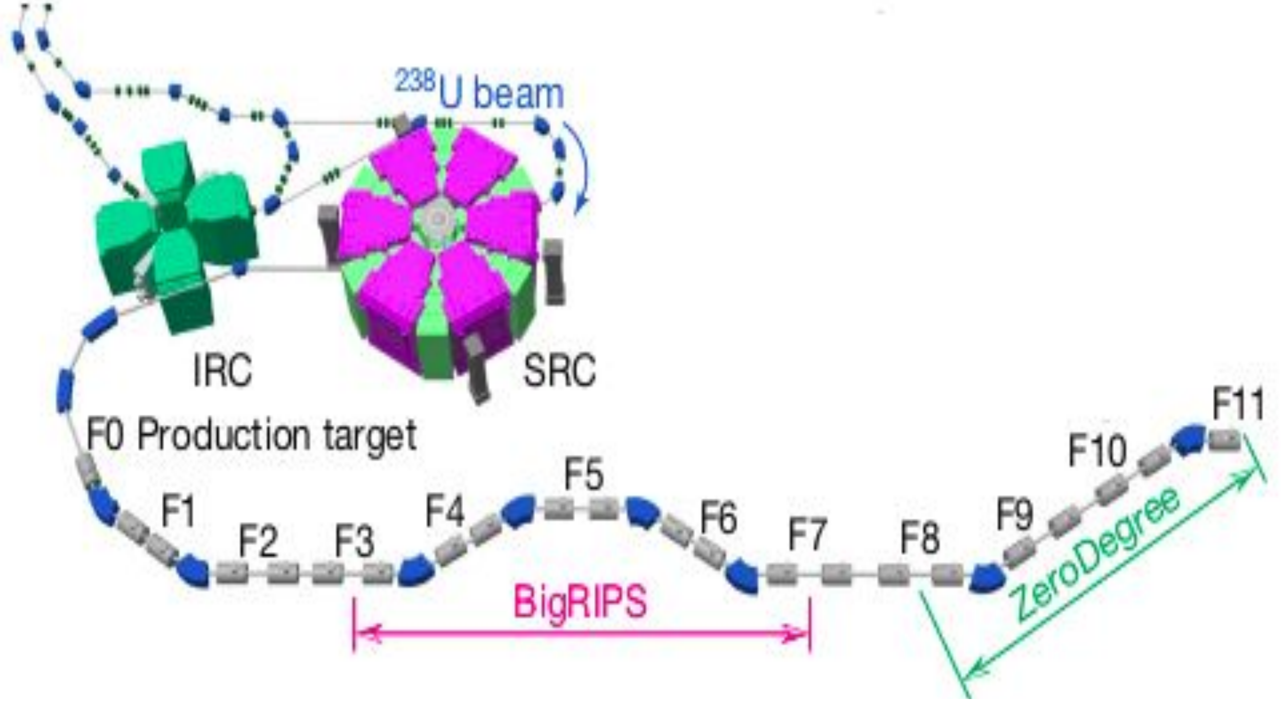

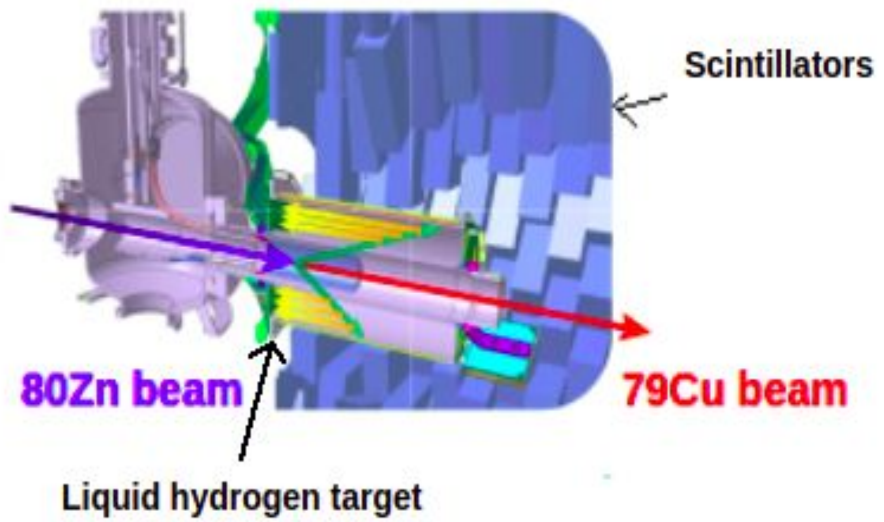

1. Introduction
1.2. Current state of knowledge

Results:

+ 11 transitions were observed.
+ A proposed level scheme up to 4.6 MeV of excitation energy.
- Some transitions are to be confirmed (weak statistics and bad energy resolution of the scintillators)

1. Introduction
1.2. Current state of knowledge

Results:

+ 11 transitions were observed.
+ A proposed level scheme up to 4.6 MeV of excitation energy.
- Some transitions are to be confirmed (weak statistics and bad energy resolution of the scintillators)

→ **New measurement proposed (HiCARI April 2021):**

+ Availability of more intense beams.
+ Use of HiCARI (High-resolution Cluster Array at RIBF) Ge array instead of scintillators
- Secondary beam of 9Be. →

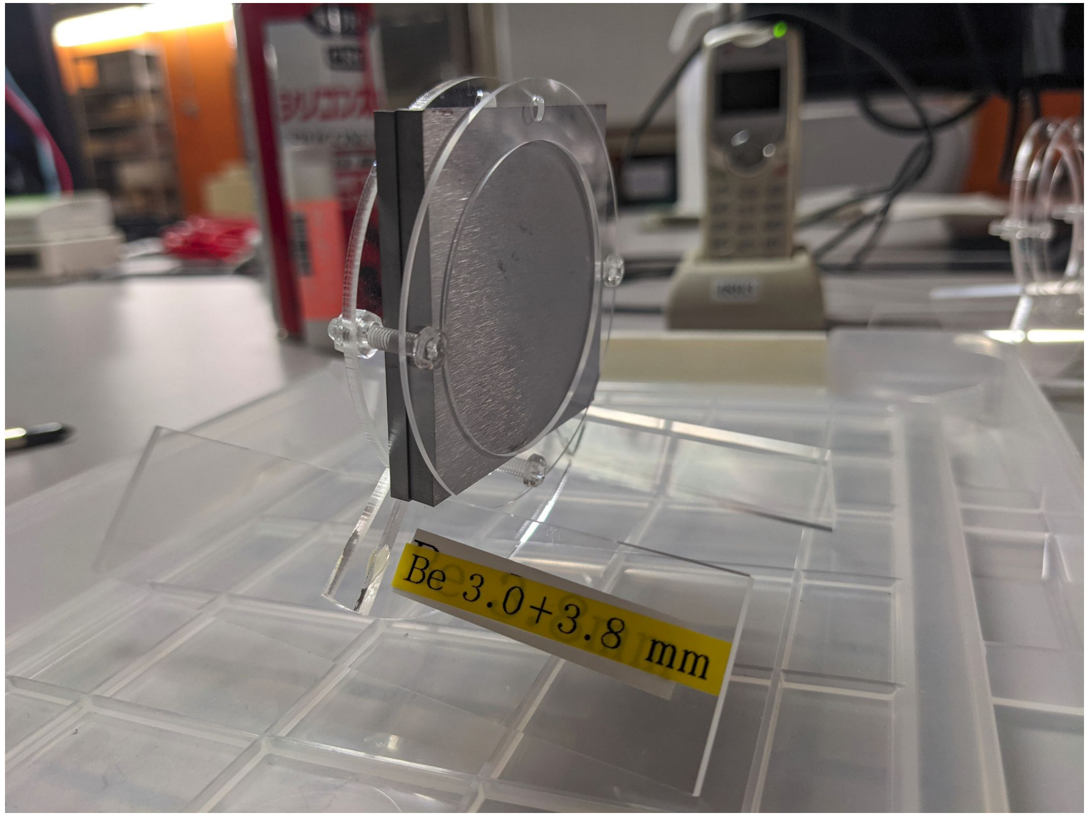

Thank you for listening

Thank you for listening to the first part

2. Data analysis
2.1. Particle Identification of the beam nuclei

We need:
$^{80}Zn(^{9}Be, X)^{79}Cu$ reaction channel
i.e:

- Gate on ^{80}Zn in BigRIPS (before the target)
- Gate on ^{79}Cu in ZeroDegree (after the target)
- Look at the corresponding γ-spectrum in coincidence

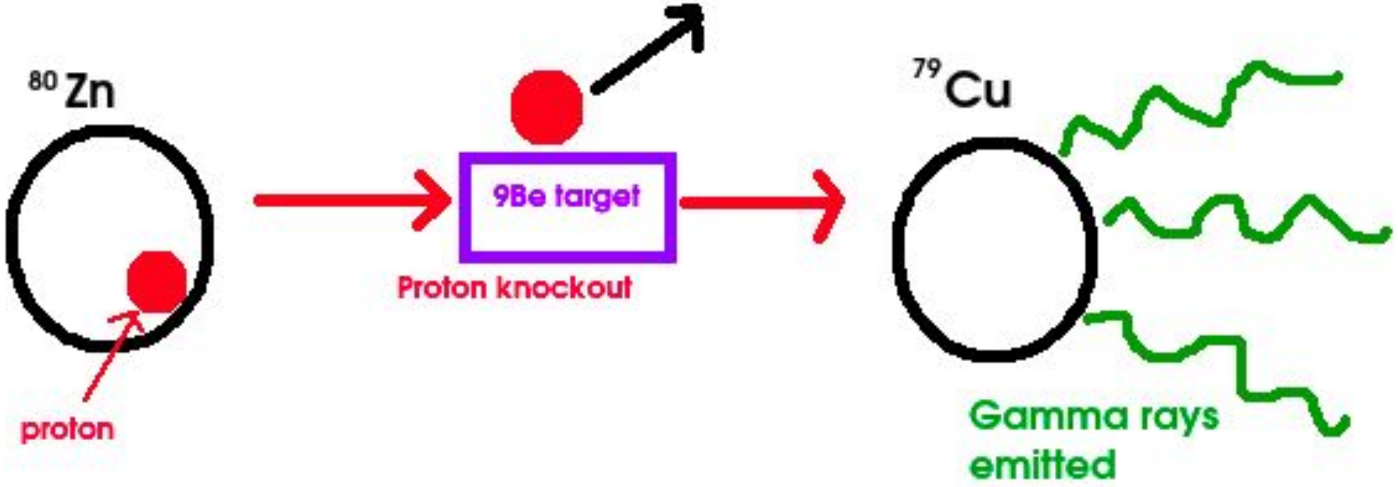

2. Data analysis
2.1. Particle Identification of the beam nuclei

We need: $^{80}Zn(^{9}Be, X)\,^{79}Cu$
- The atomic number Z.
- The mass number A (or equivalently A/Q).

$$\frac{A}{Q} = \frac{B\rho}{\beta\gamma}\frac{c}{m_u}$$

$$\frac{dE}{dx} = \frac{4\pi e^4 Z^2}{m_e v^2} N z \left[\ln\frac{2m_e v^2}{I} - \ln\left(1-\beta^2\right) - \beta^2\right]$$

$$\mathrm{TOF} = \frac{L}{\beta c}$$

Example in BigRIPS separator

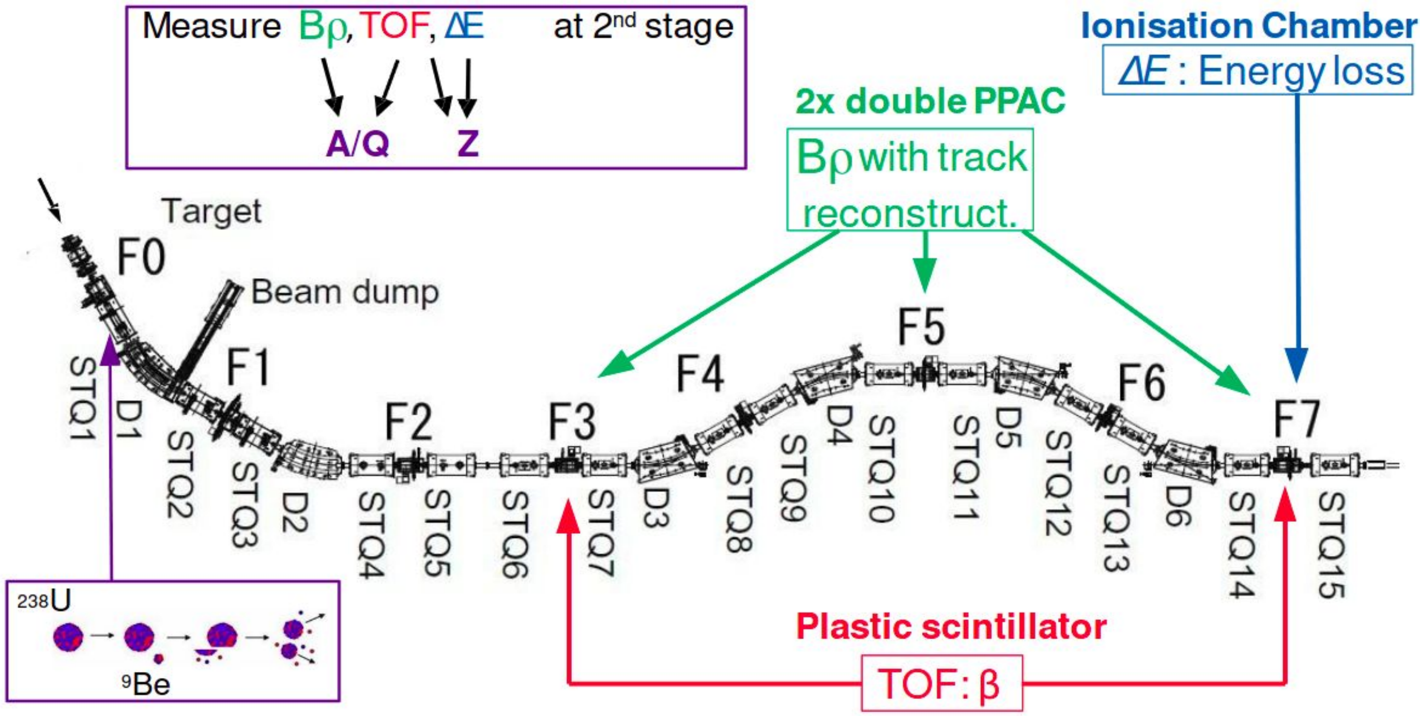

2. Data analysis
2.1. Particle Identification of the beam nuclei

Result:

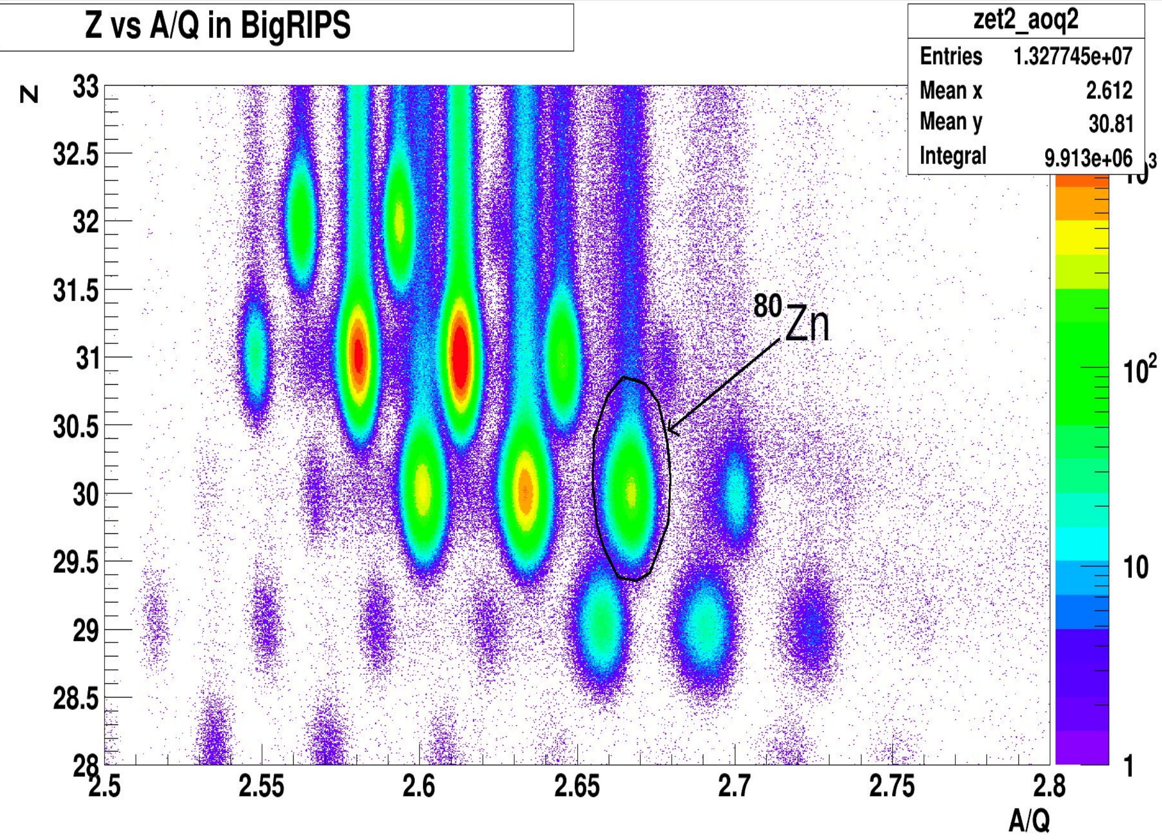

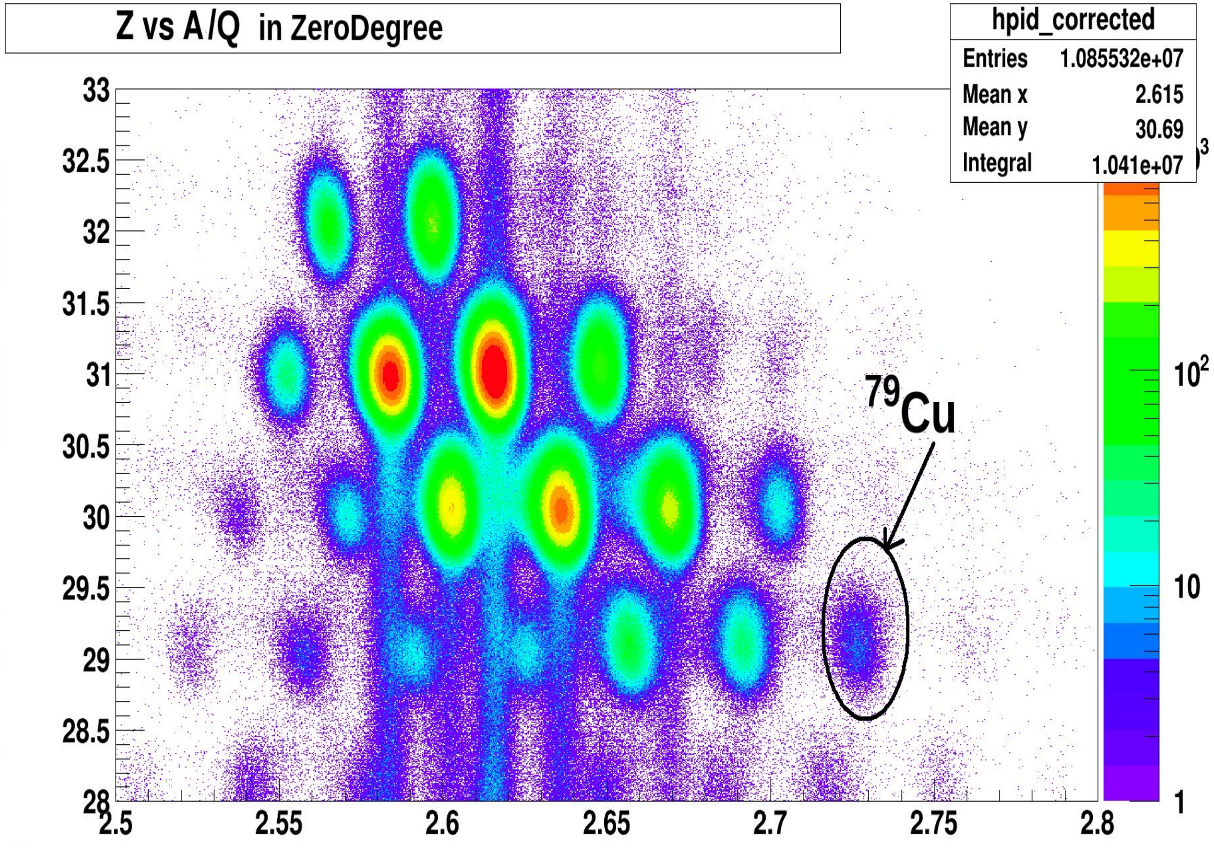

2. Data analysis
2.2. Energy calibration of HiCARI Ge array

Purpose:
Find the linear relation between the voltage of the collected current and the energy deposit of the γ-ray.
E(keV) = a* E(ADC) + b

We used sources of 60Co, 152Eu, 88Y and 133Ba.

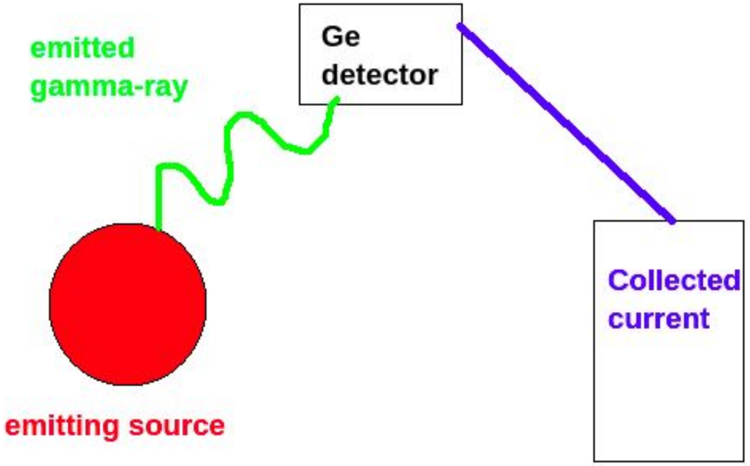

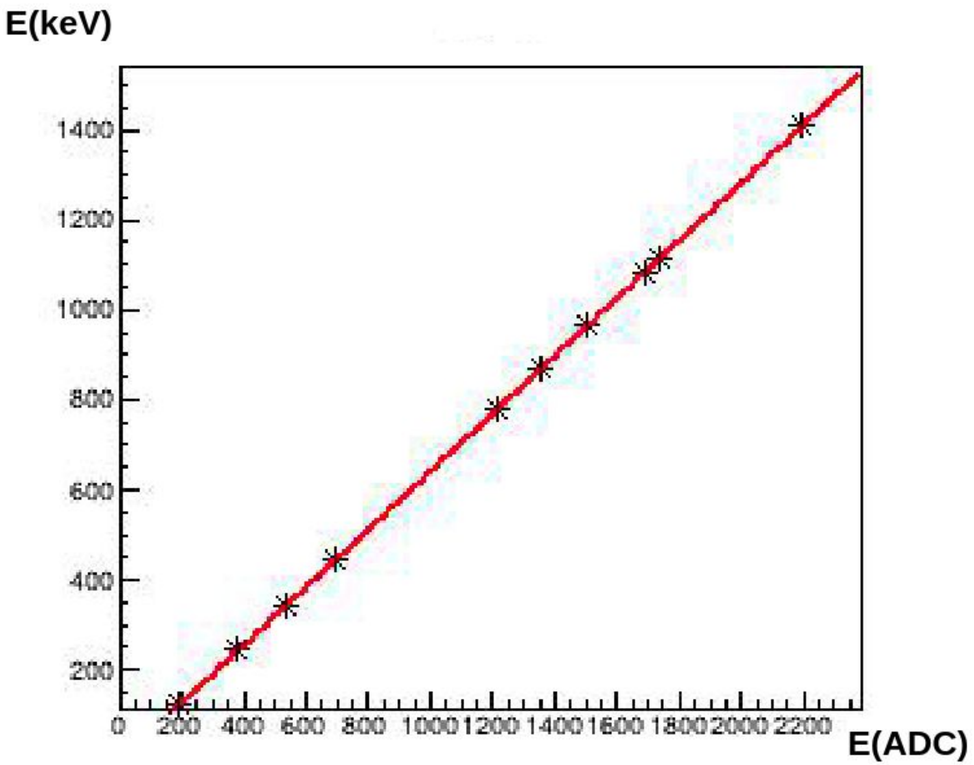

2. Data analysis
2.2. Energy calibration of HiCARI Ge array

Purpose:
Find the linear relation between the voltage of the collected current and the energy deposit of the γ-ray.

Example:
With ^{60}Co source

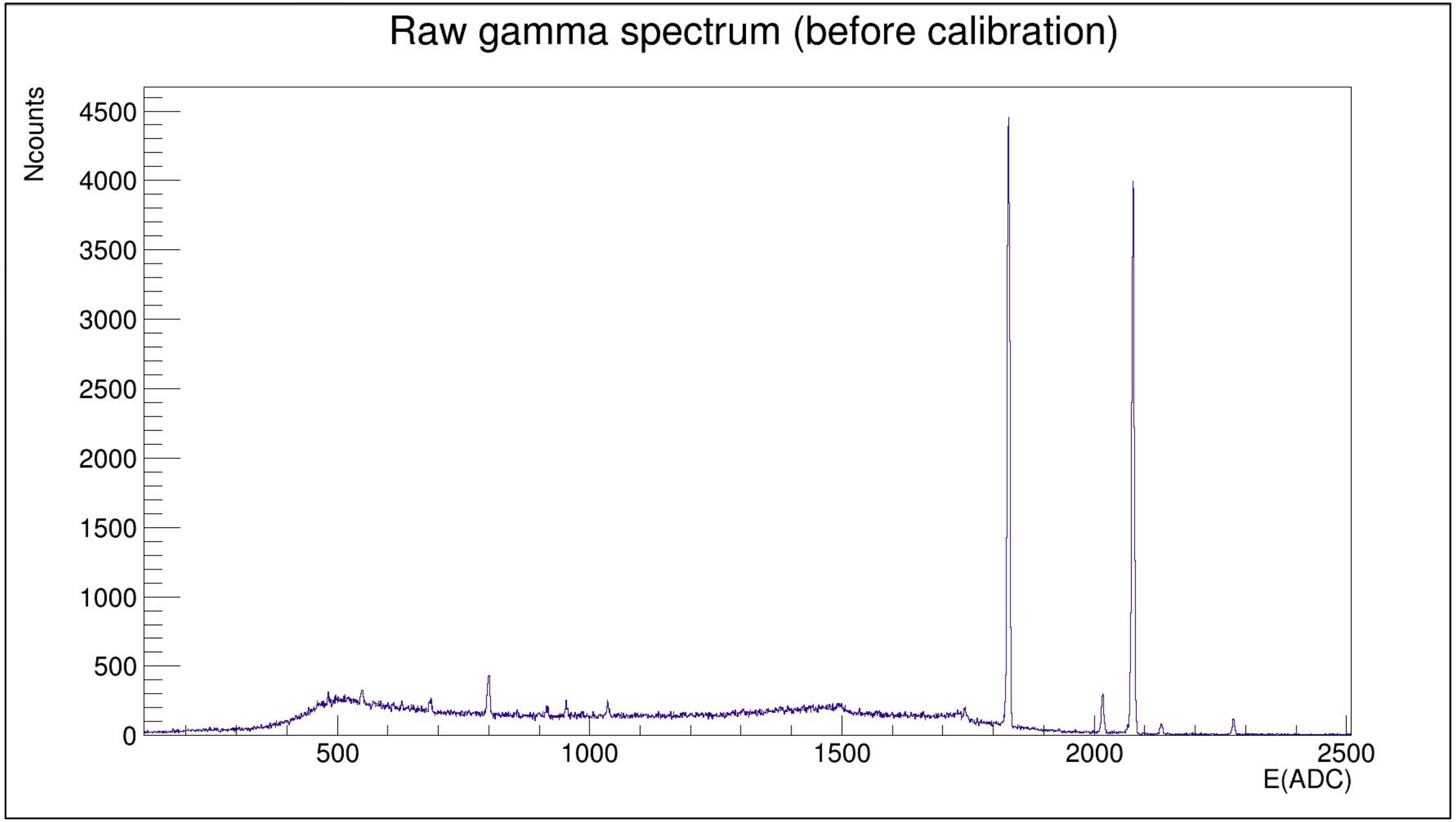

2. Data analysis
2.2. Energy calibration of HiCARI Ge array

Purpose:
Find the linear relation between the voltage of the collected current and the energy deposit of the γ-ray.

Example:
With ^{60}Co source

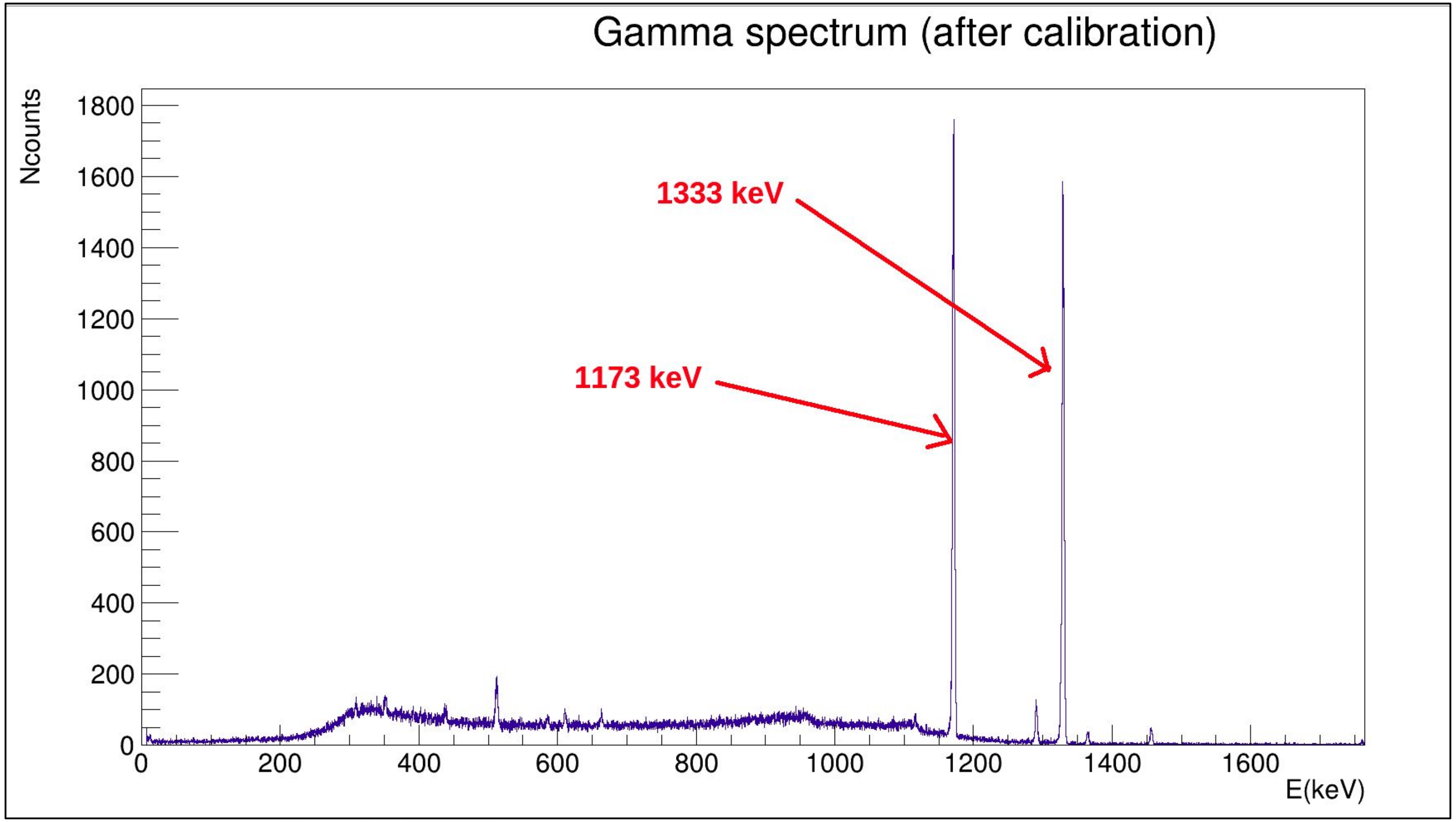

2. Data analysis
2.3. Velocity determination

^{79}Cu nuclei have relativistic velocities:

- We need to correct for the Doppler shift.

$$E_0 = E_\gamma \frac{1 - \beta \cos\theta}{\sqrt{1-\beta^2}}$$

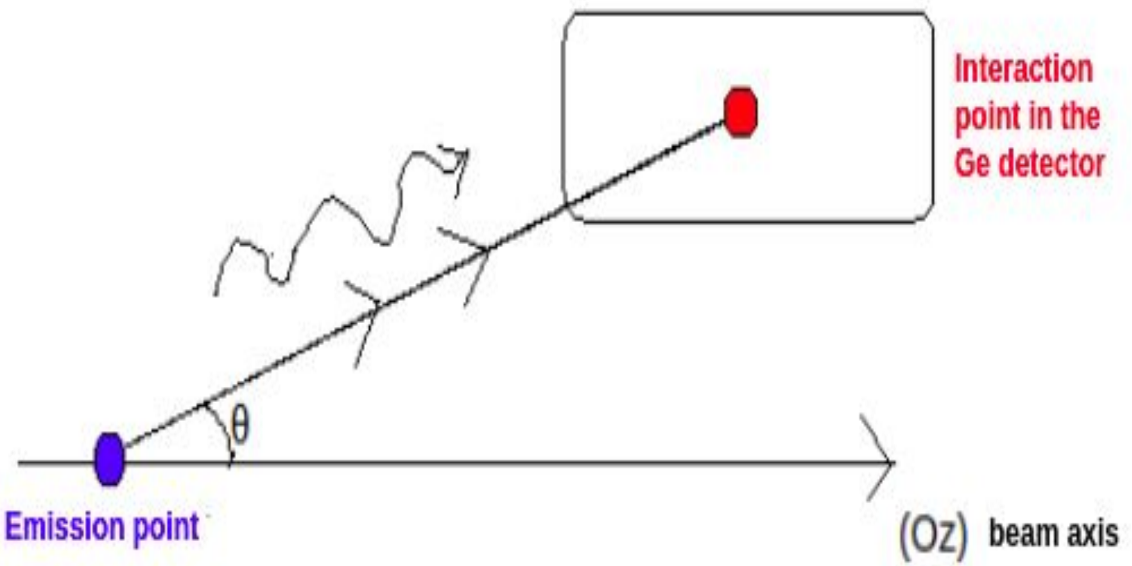

Eo : Energy of the γ-ray in the rest frame of the emitting nucleus.
E_γ : Energy of the γ-ray in the laboratory frame.

2. Data analysis
2.3. Velocity determination

^{79}Cu nuclei have relativistic velocities:

- We need to correct for the Doppler shift.

$$E_0 = E_\gamma \frac{1 - \beta \cos\theta}{\sqrt{1-\beta^2}}$$

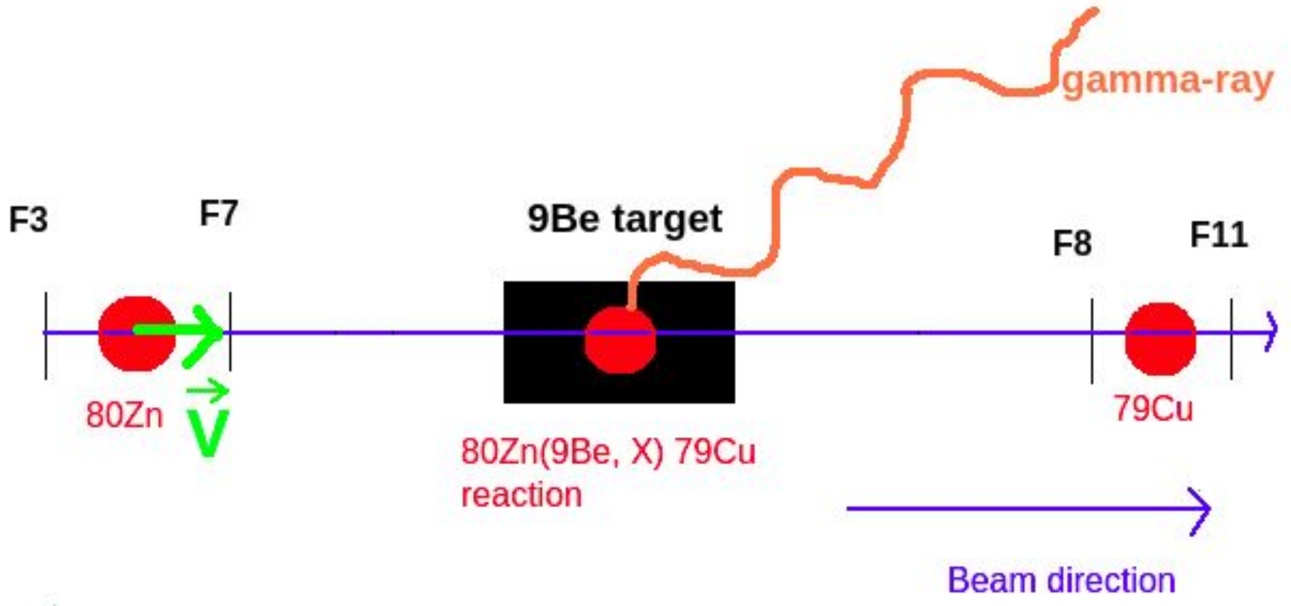

Eo : Energy of the γ-ray in the rest frame of the emitting nucleus.

E_γ : Energy of the γ-ray in the laboratory frame.

2. Data analysis
2.3. Velocity determination

^{79}Cu nuclei have relativistic velocities:
- We need to correct for the Doppler shift.

$$E_0 = E_\gamma \frac{1 - \beta \cos\theta}{\sqrt{1 - \beta^2}}$$

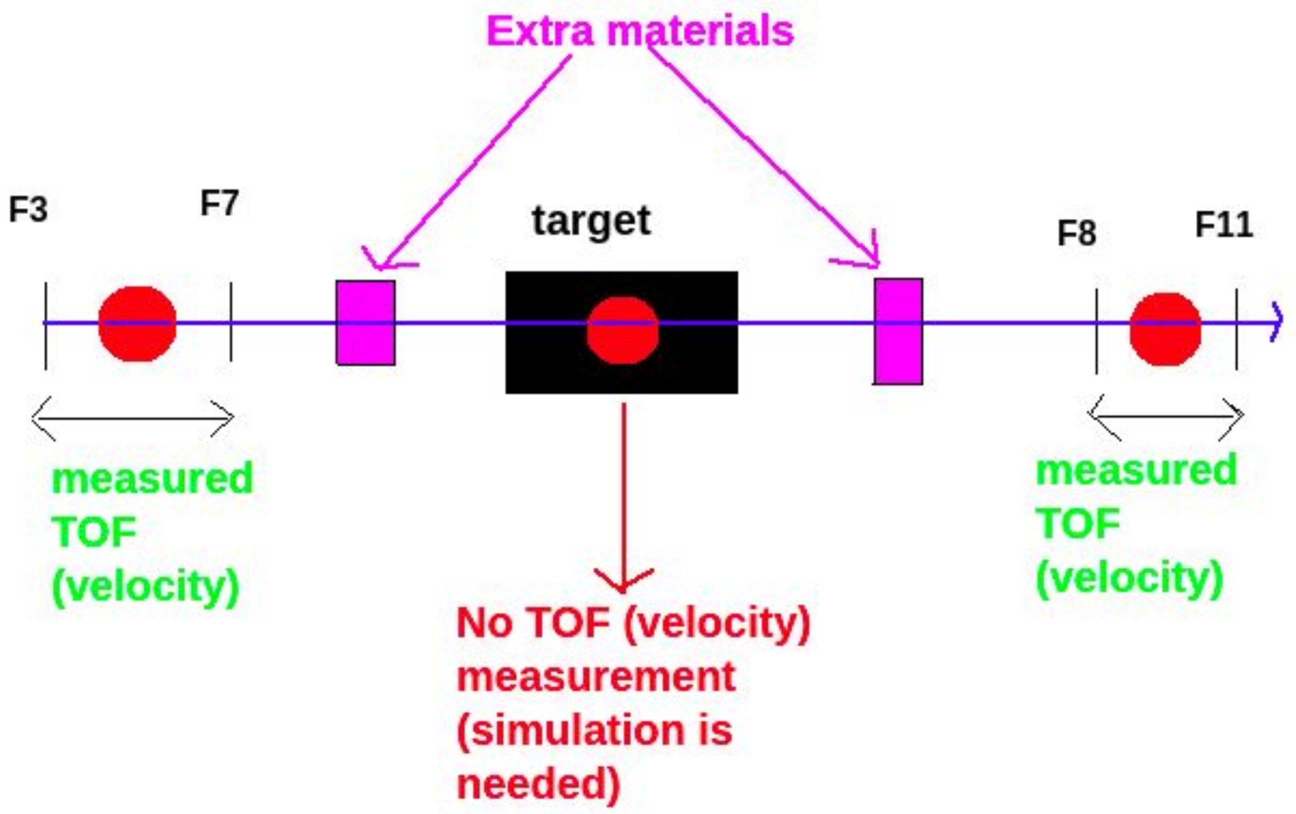

Eo : Energy of the γ-ray in the rest frame of the emitting nucleus.
E_γ : Energy of the γ-ray in the laboratory frame.

2. Data analysis
2.3. Velocity determination

^{79}Cu nuclei have relativistic velocities:

- We estimate the velocity at the target center using LISE++ simulation.

β[F3-F7] DATA	β at center LISE++ simulation	β (F8-F11) LISE++ simulation	β[F8-F11] DATA	difference
0.6284	0.6027	0.5806	0.5796	0.0010 (0.18%)

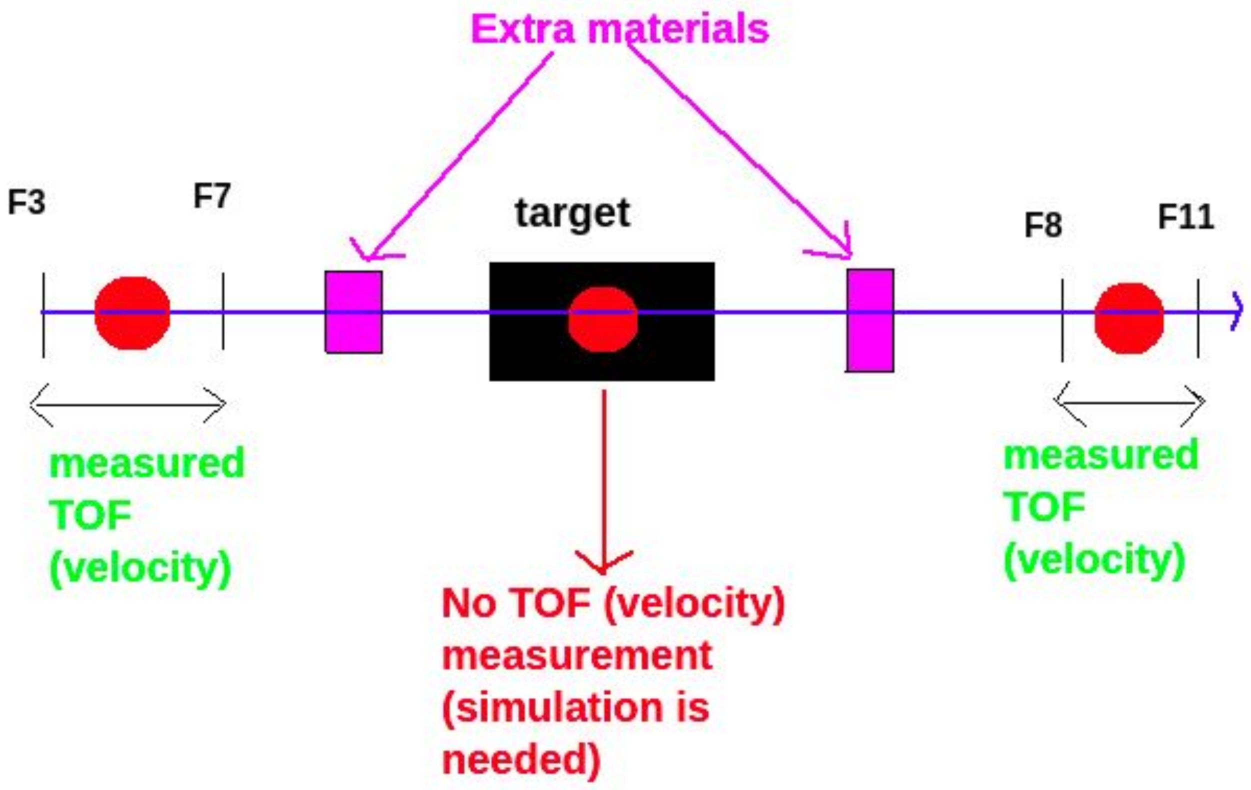

2. Data analysis
2.4. Preliminary Doppler-corrected gamma-spectra

- In the HiCARI Ge array:
  + 4 Miniballs
  + 4 Clovers
  + 1 P3
  + 1 QUAD

They do not have the same efficiencies and energy resolutions.

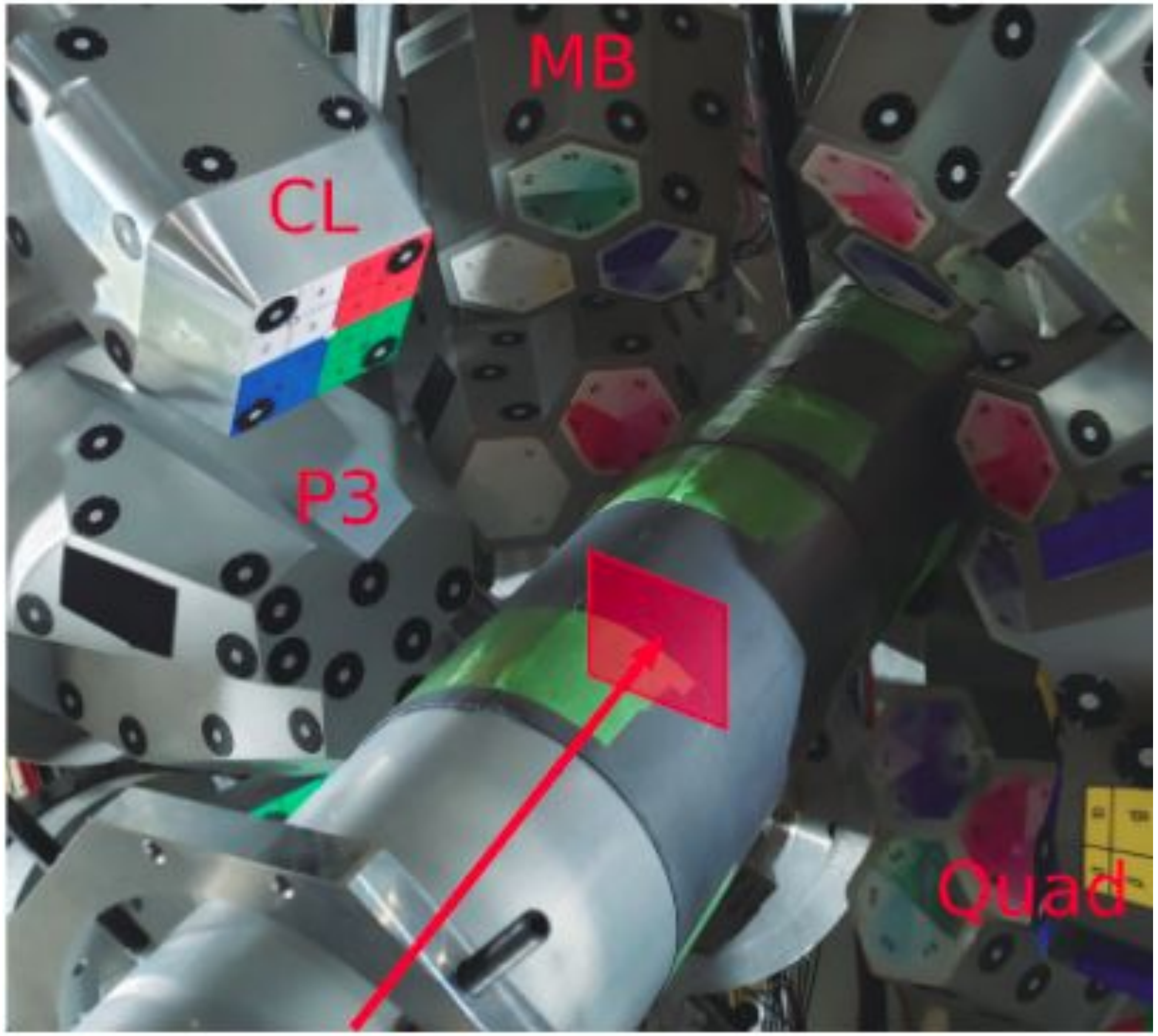

2. Data analysis
2.4. Preliminary Doppler-corrected gamma-spectra

- In the HiCARI Ge array:
+ 4 Miniballs
+ 4 Clovers
+ 1 P3
+ 1 QUAD

They do not have the same efficiencies and energy resolutions.

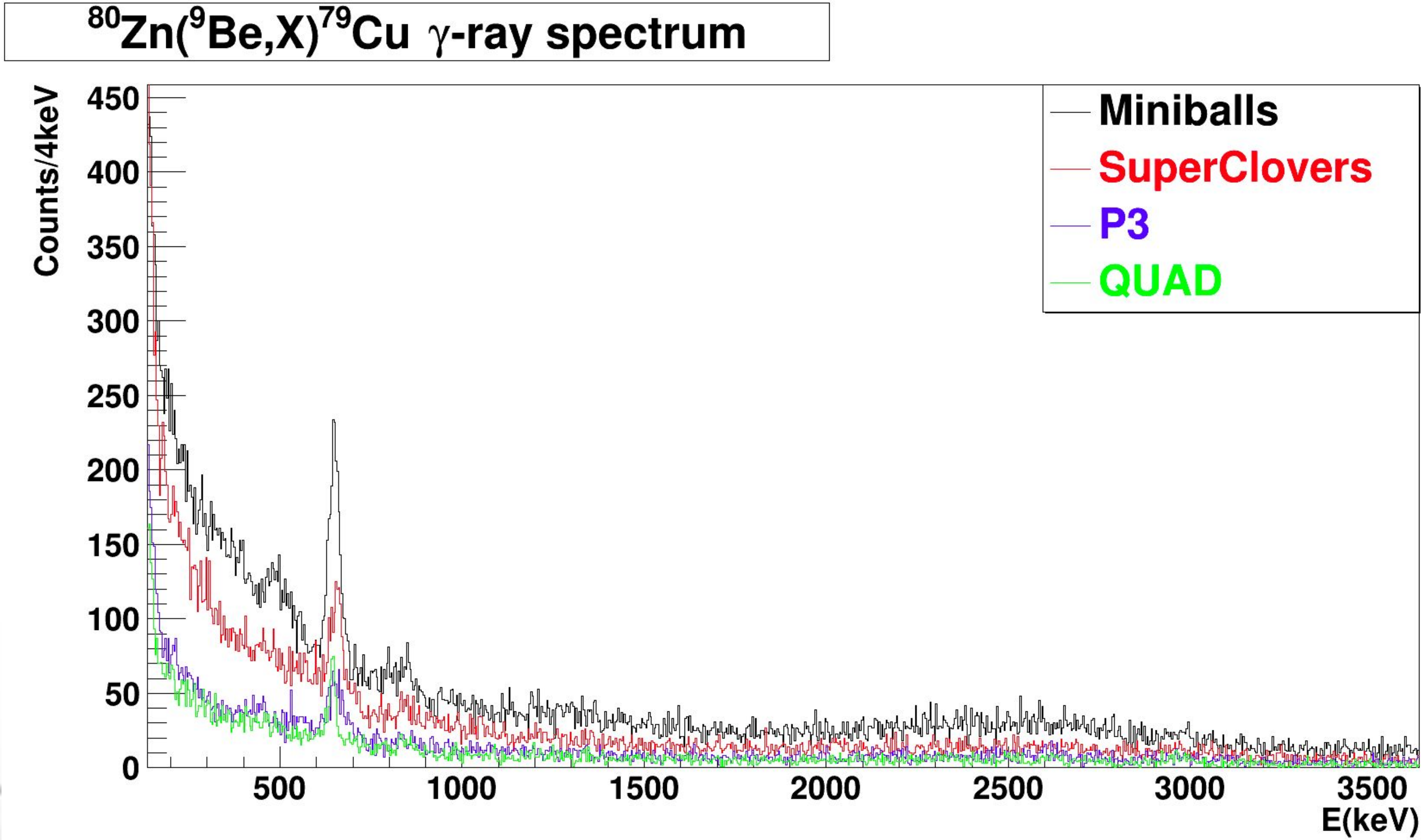

2. Data analysis
2.4. Preliminary Doppler-corrected gamma-spectra

Example with SuperClovers:

+ We can see some of the peaks from the previous SEASTAR campaign.

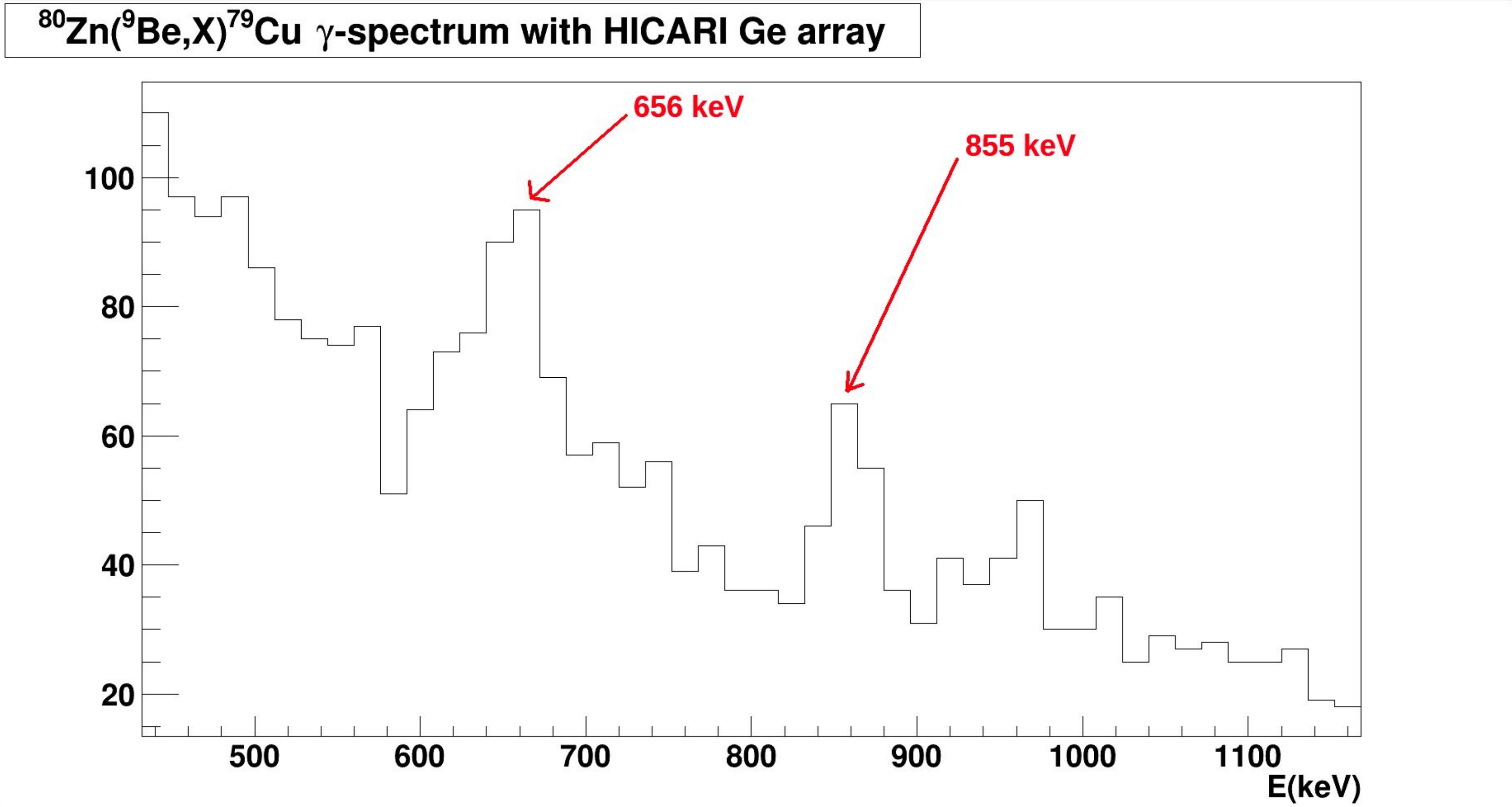

2. Data analysis
2.4. Preliminary Doppler-corrected gamma-spectra

Looking at the mean and width of the peaks:
Example with Miniball
E= 649 ± 1 keV
Almost in agreement with the SEASTAR result:
E = 656 ± 5 keV

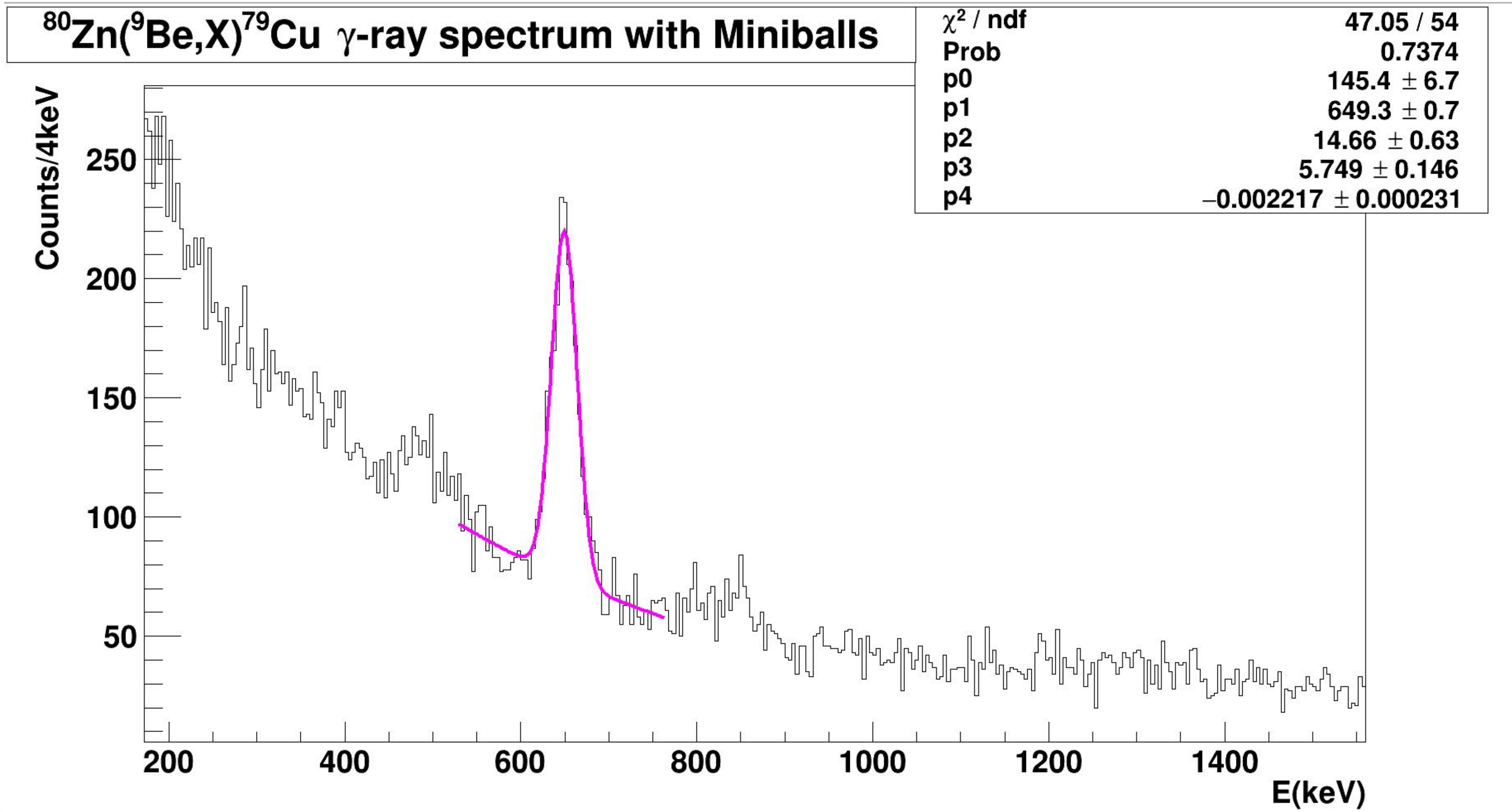

2. Data analysis

2.4. Preliminary Doppler-corrected gamma-spectra

Main issue:
We get different mean values depending on the detector type

Detector(s)	E (keV)	Error (keV)
Miniballs	649	1
SuperClovers	656	2
P3	656	3
QUAD	644	1

2. Data analysis

2.4. Preliminary Doppler-corrected gamma-spectra

Possible reasons for the energy shifts:

- Wrong angle in the doppler correction due to the geometry (positions of detectors and/or target).

$$E_0 = E_\gamma \frac{1 - \beta \cos\theta}{\sqrt{1 - \beta^2}}$$

2. Data analysis

2.4. Preliminary Doppler-corrected gamma-spectra

Possible reasons for the energy shifts:

- Wrong angle in the doppler correction due to the geometry (positions of detectors and/or target).
- Lifetime effect:

$\theta < \theta real$

Eo < Eo (real)

$$E_0 = E_\gamma \frac{1 - \beta \cos \theta}{\sqrt{1 - \beta^2}}$$

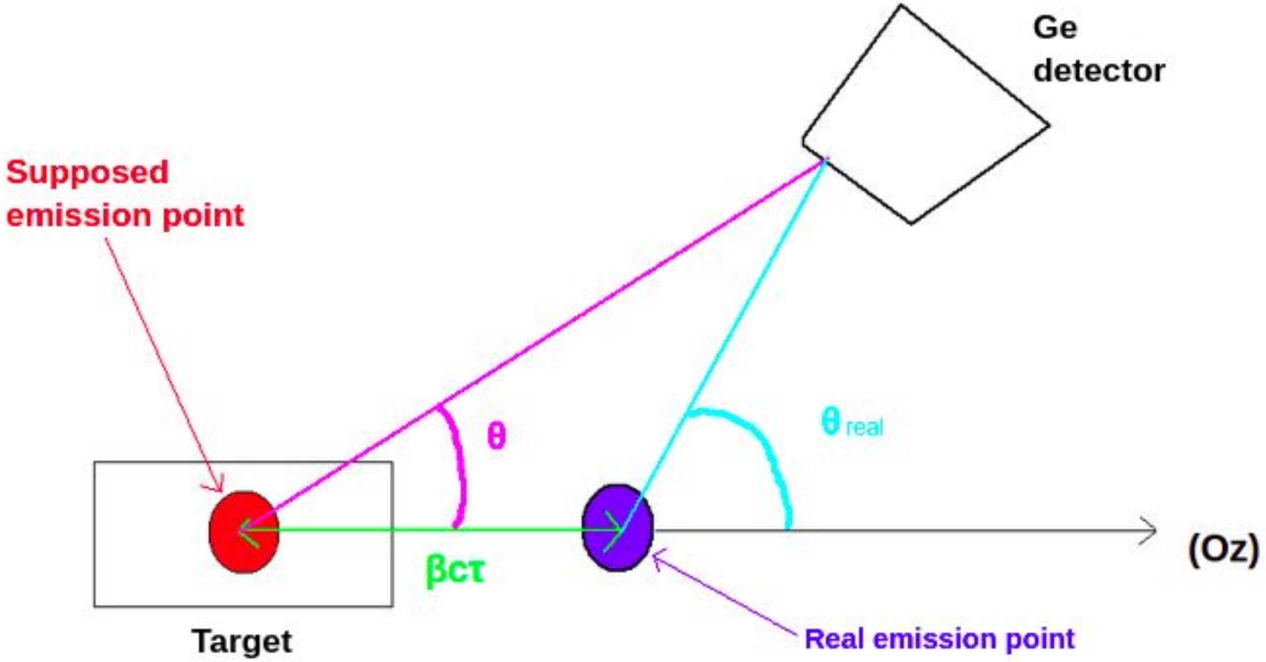

3. Conclusion and outlook

- Solve the energy shifts issue: Shift the target position until finding the best agreement between the energies.
- Run GEANT4 simulations to check for the possible lifetime effects.
- Apply ɣɣ coïncidences

Thank you for your attention

Annexes

1- Relation between pnA and pps:

ϕ(pps) * (1.6 e) = ϕ' (pA)

ϕ(pps) * (1.6 e) * 10^9 = ϕ'' (pnA)

Beam intensity (^{238}U) = 90 pnA = 5.625 * 10^{11}pps

Total beam intensity at F7 = 4 * 10^4 pps

2- Energy resolutions comparison from simulation

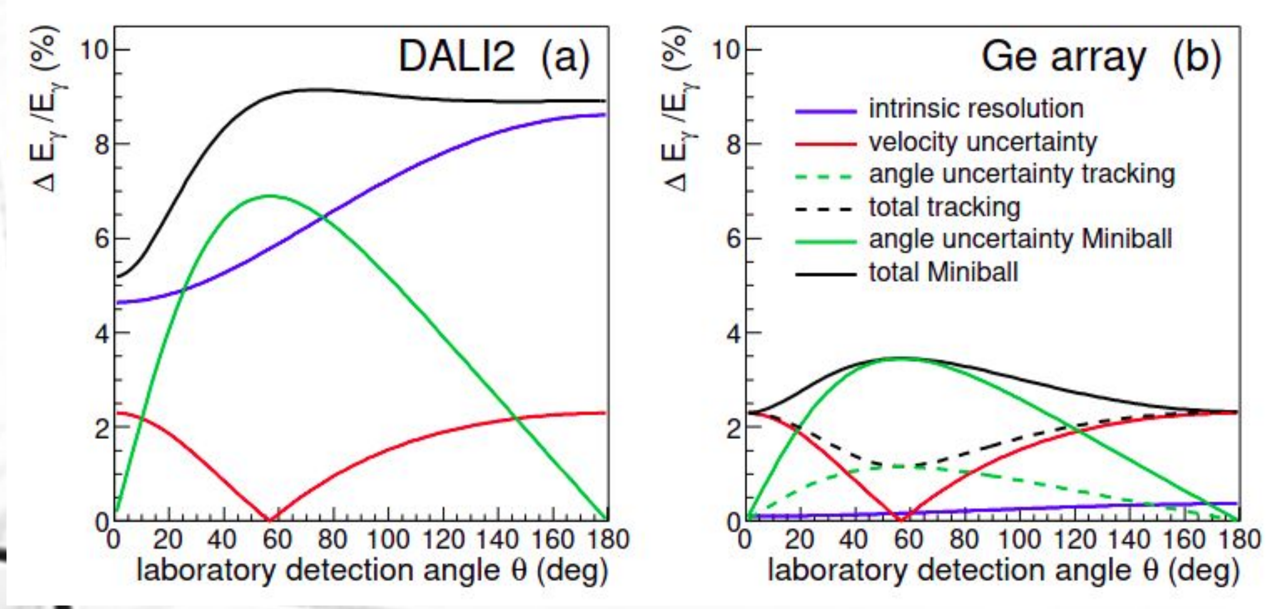

2. Data analysis
2.1. Particle Identification of the beam nuclei

Removal of background events:

Example:
Time/charge correlation in the plastic scintillators:
$T_R - T_L = A \log(q_L/q_R)$
at F3, F7, F8 and F11.

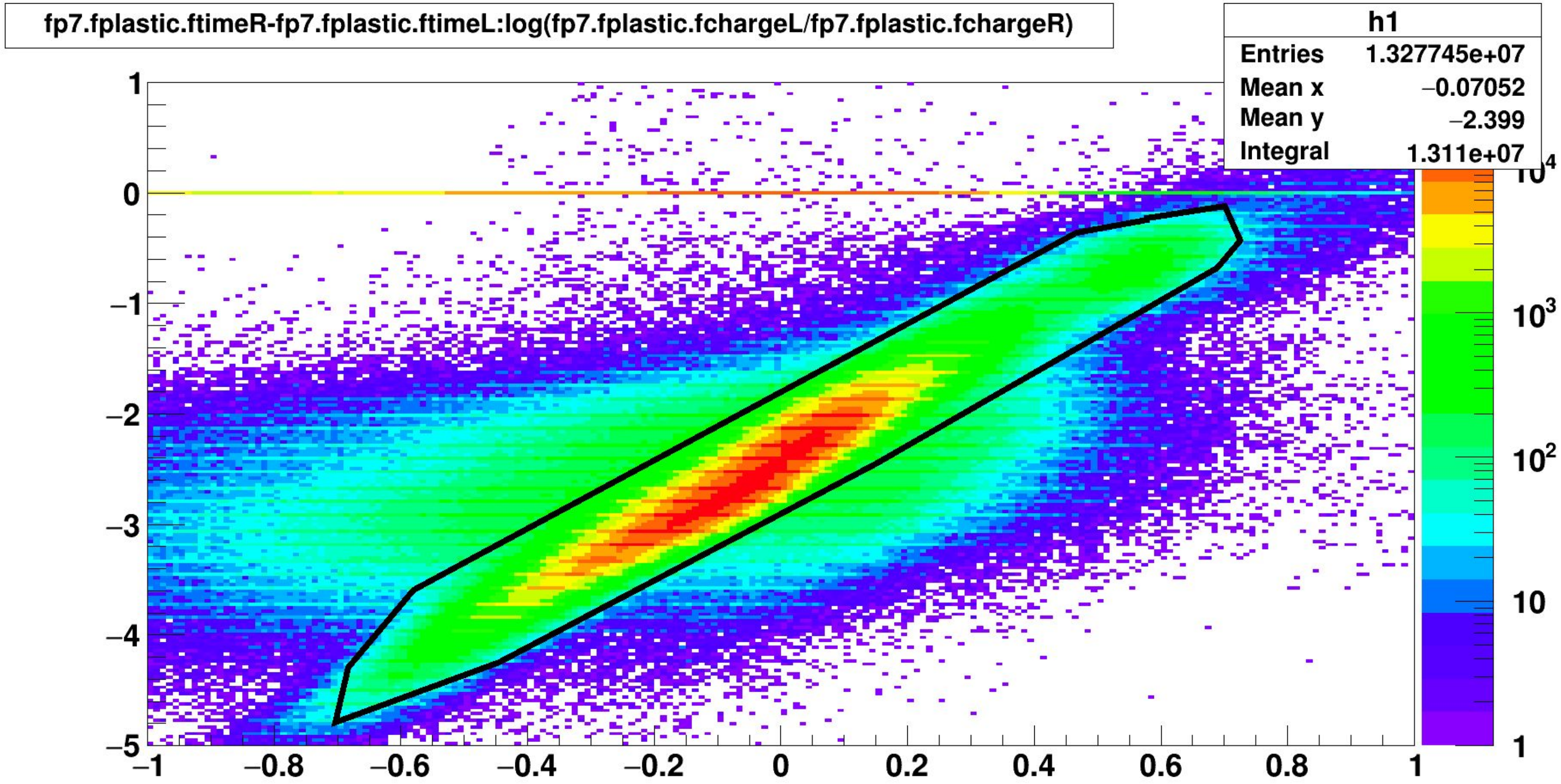

2. Data analysis
2.1. Particle Identification of the beam nuclei

Optical corrections:
Cancel the A/Q dependency on position and angular variables, in order to achieve a better resolution for the A/Q.

Example: A/Q vs the angular variable “a” at focal plane 5.

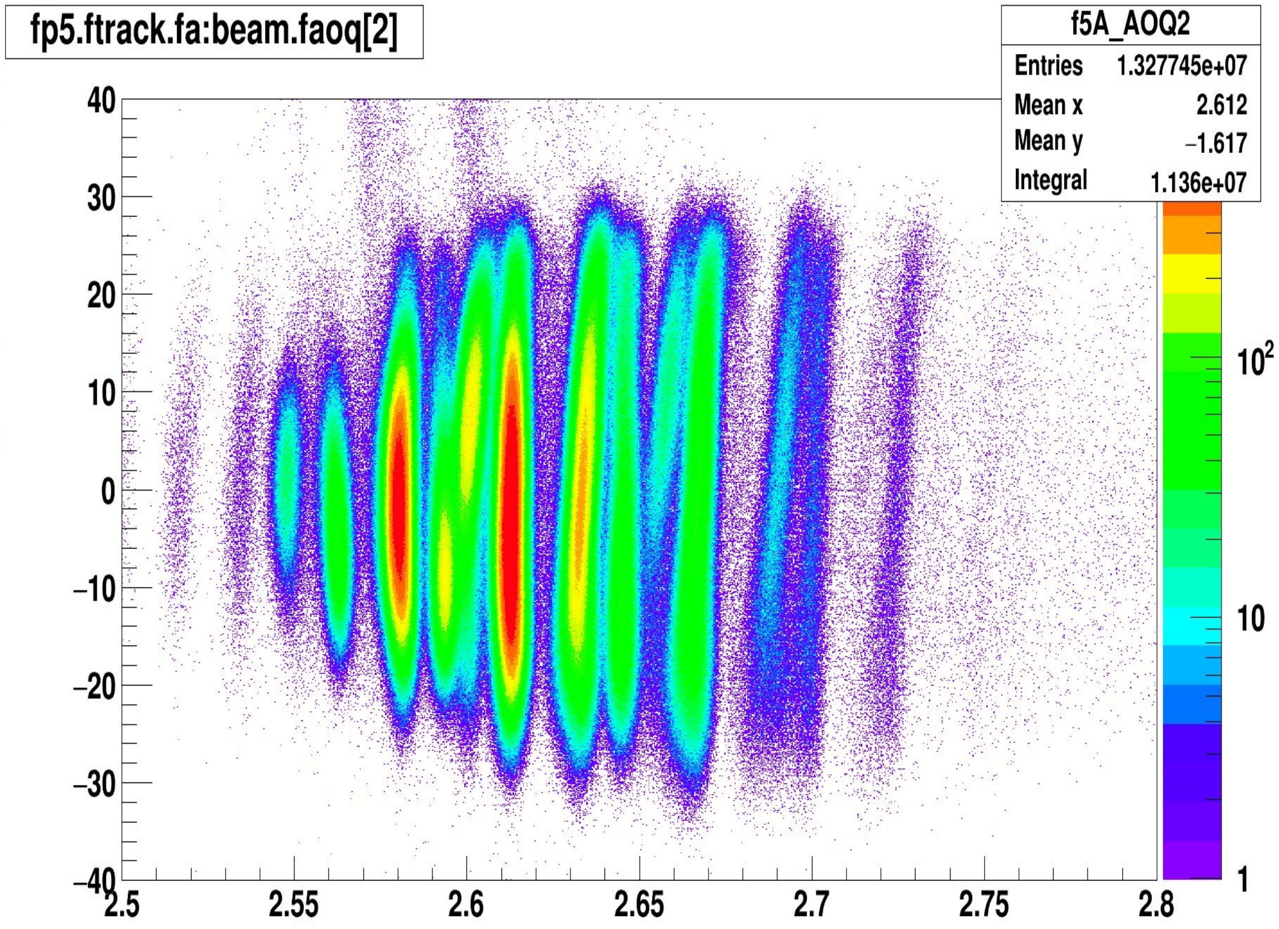

2. Data analysis
2.1. Particle Identification of the beam nuclei

<u>Optical corrections:</u>
Cancel the A/Q dependency on position and angular variables, in order to achieve a better resolution for the A/Q.

<u>Example:</u> A/Q vs the angular variable “a” at focal plane 5.

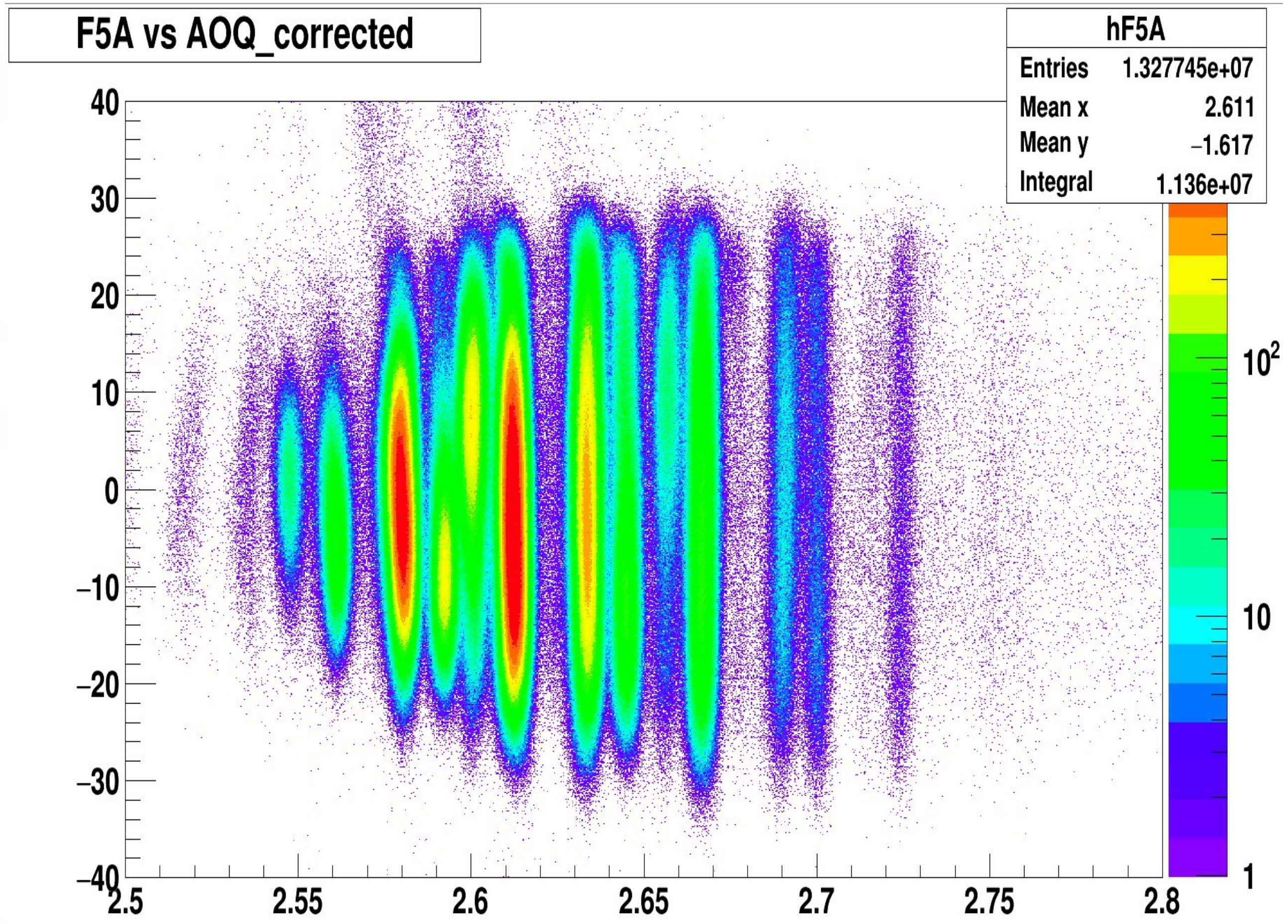

Detector(s)	E (keV)	Error (keV)
Miniball_0	651	3
Miniball_2	646	4
Miniball_4	651	1
Miniball_5	650	1

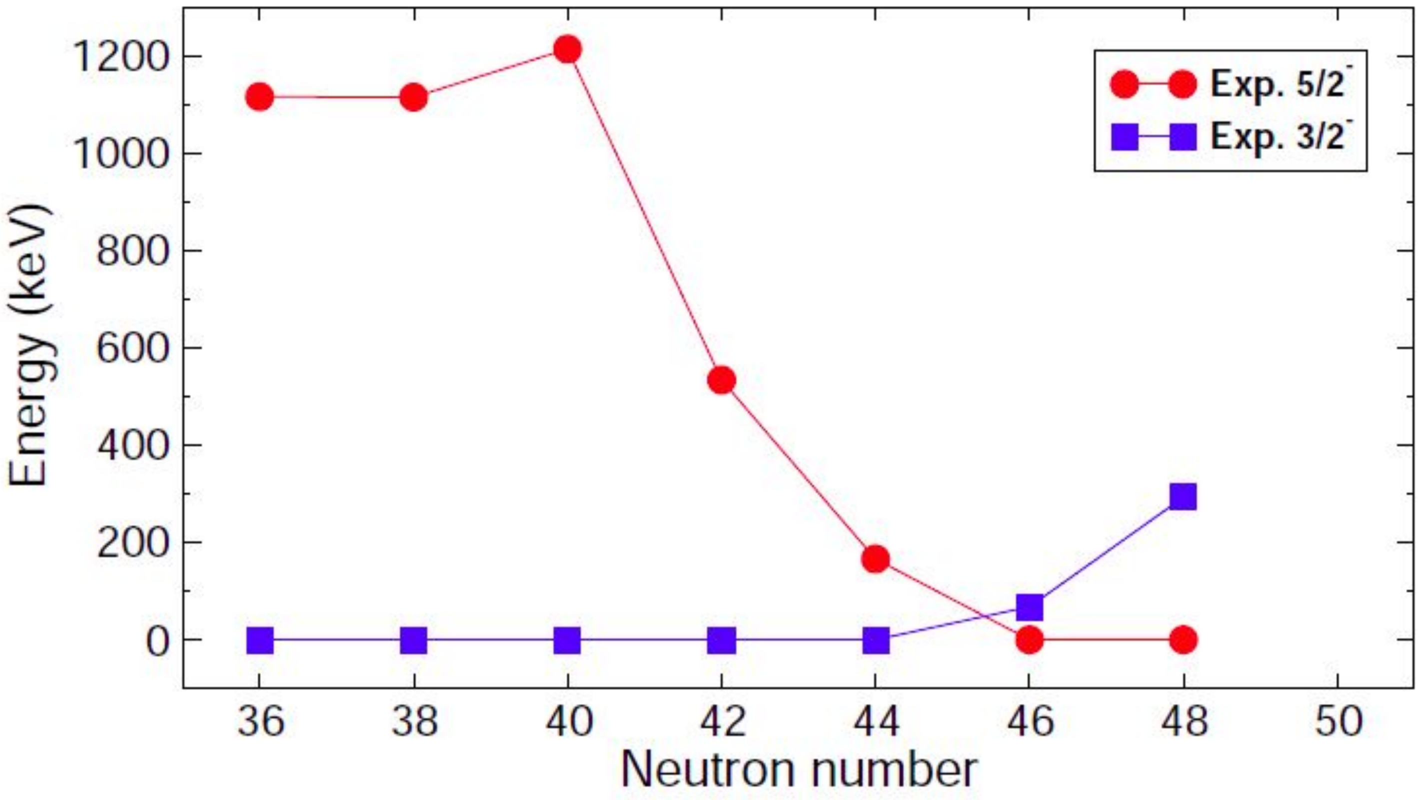

Figure 1.6 – Systematics of the first $3/2^-$ and $5/2^-$ states in neutron-rich copper isotopes. The ground-state spin changes at $N = 46$. Data taken from references [26, 43, 46–50].

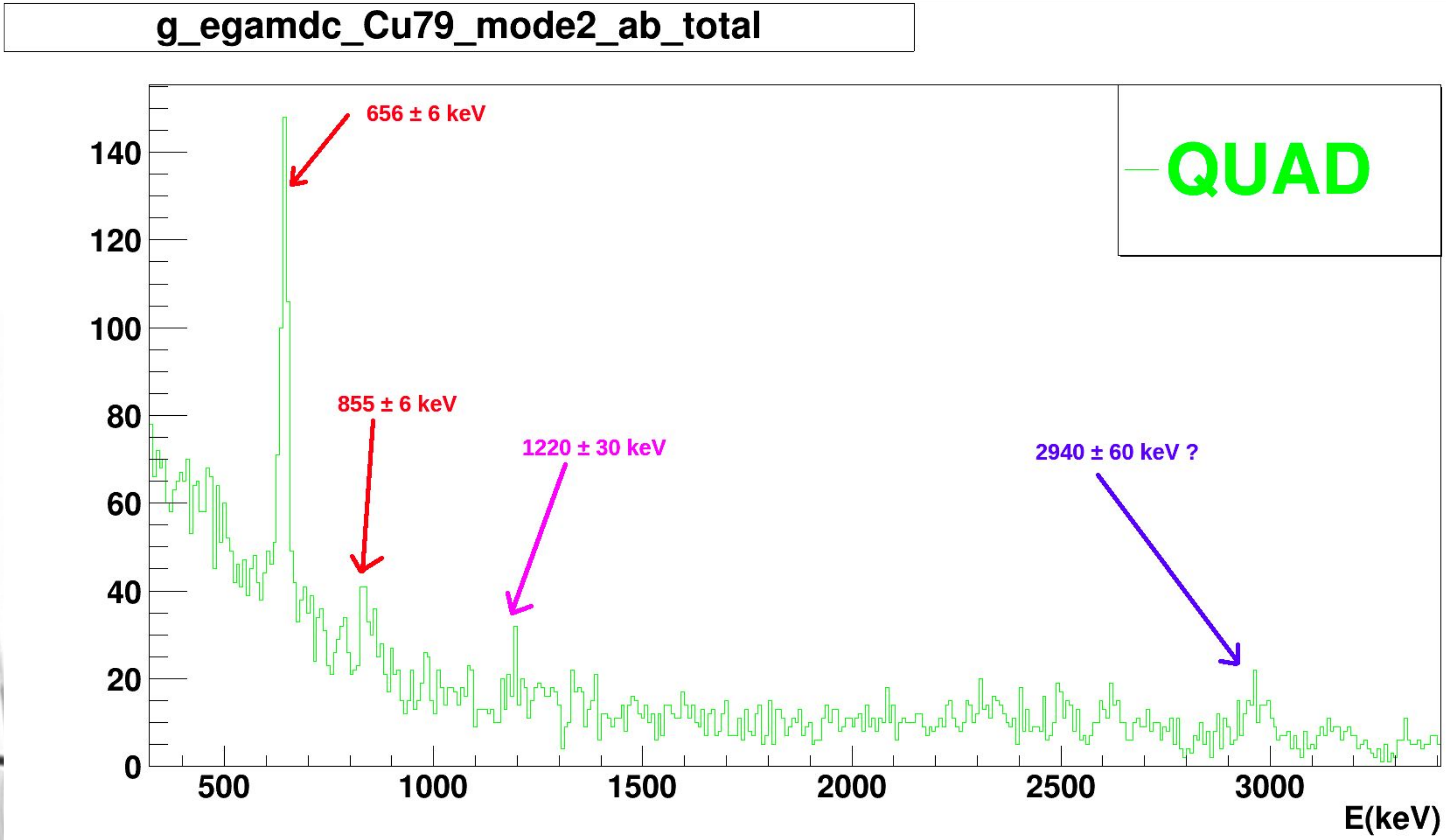

g_egamdc_Cu79_mode2_ab_total
656 ± 6 keV
855 ± 6 keV
1220 ± 30 keV
2940 ± 60 keV ?
QUAD
0
20
40
60
80
100
120
140
500
1000
1500
2000
2500
3000
E(keV)

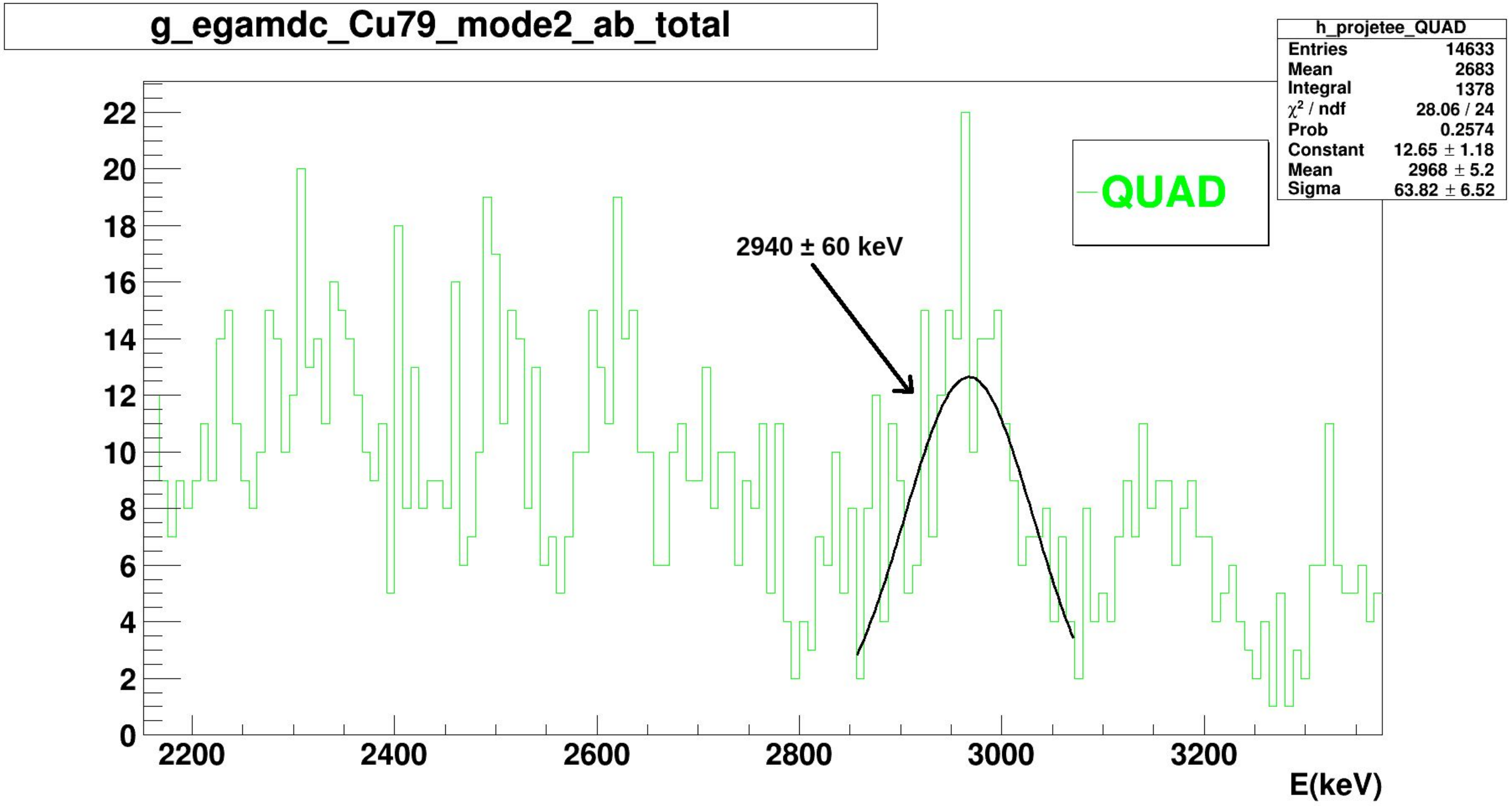

g_egamdc_Cu79_mode2_ab_total
h_projetee_QUAD
Entries 14633
Mean 2683
Integral 1378
χ² / ndf 28.06 / 24
Prob 0.2574
Constant 12.65 ± 1.18
Mean 2968 ± 5.2
Sigma 63.82 ± 6.52
QUAD
2940 ± 60 keV
0
2
4
6
8
10
12
14
16
18
20
22
2200
2400
2600
2800
3000
3200
E(keV)

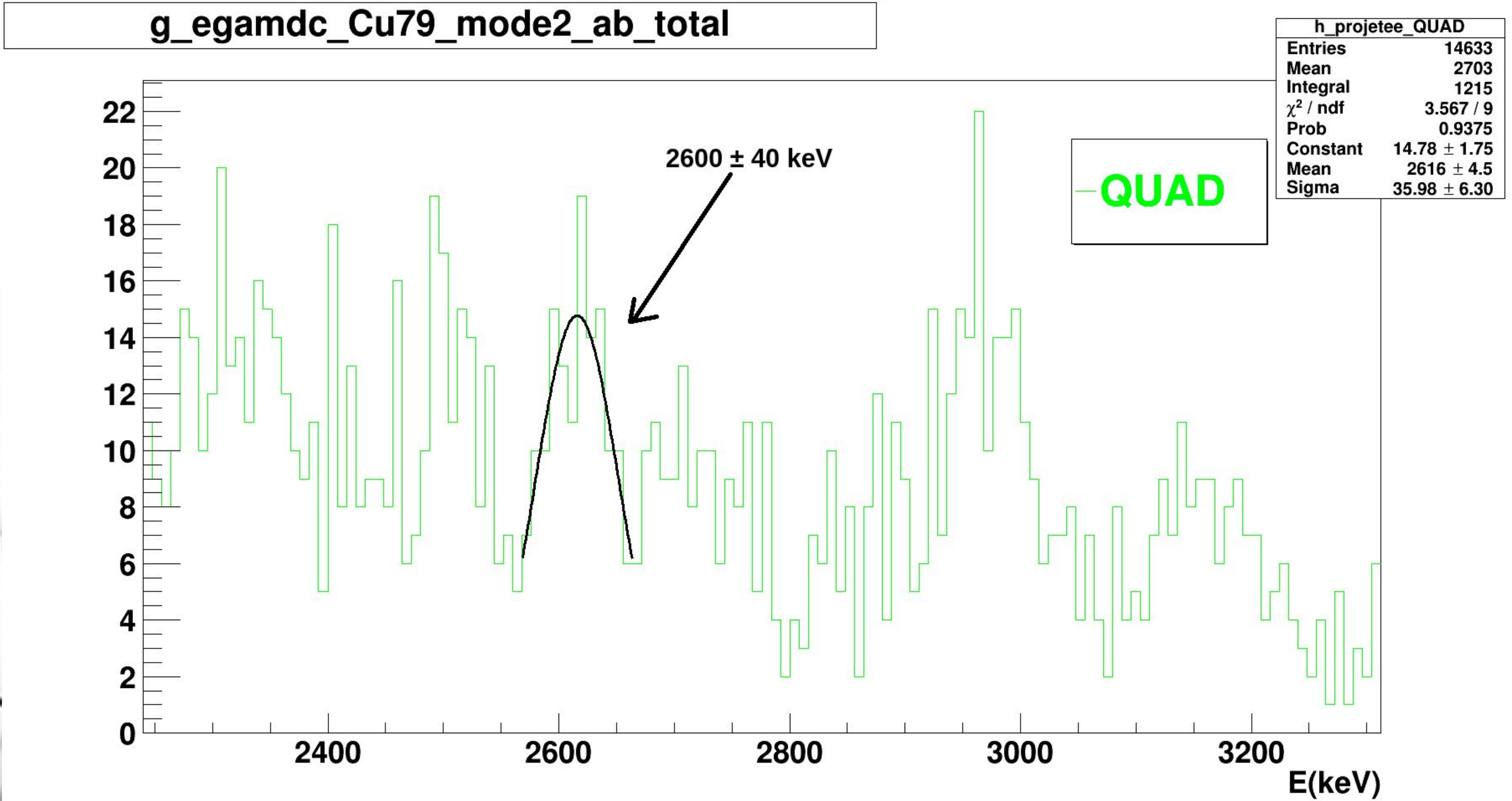
g_egamdc_Cu79_mode2_ab_total
h_projetee_QUAD
Entries 14633
Mean 2703
Integral 1215
χ^2 / ndf 3.567 / 9
Prob 0.9375
Constant 14.78 ± 1.75
Mean 2616 ± 4.5
Sigma 35.98 ± 6.30
QUAD
2600 ± 40 keV
E(keV)

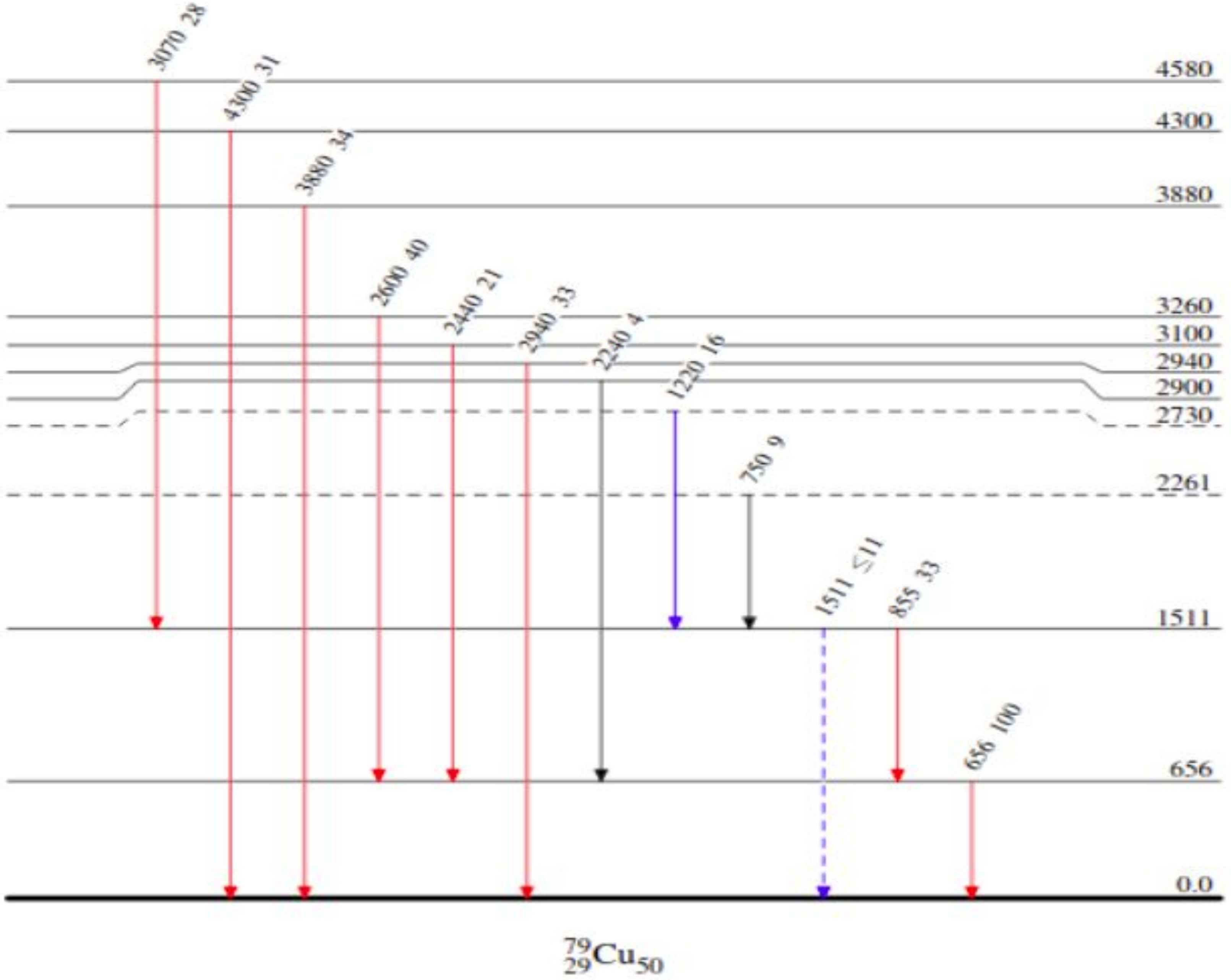

Schéma de niveaux du 79Cu

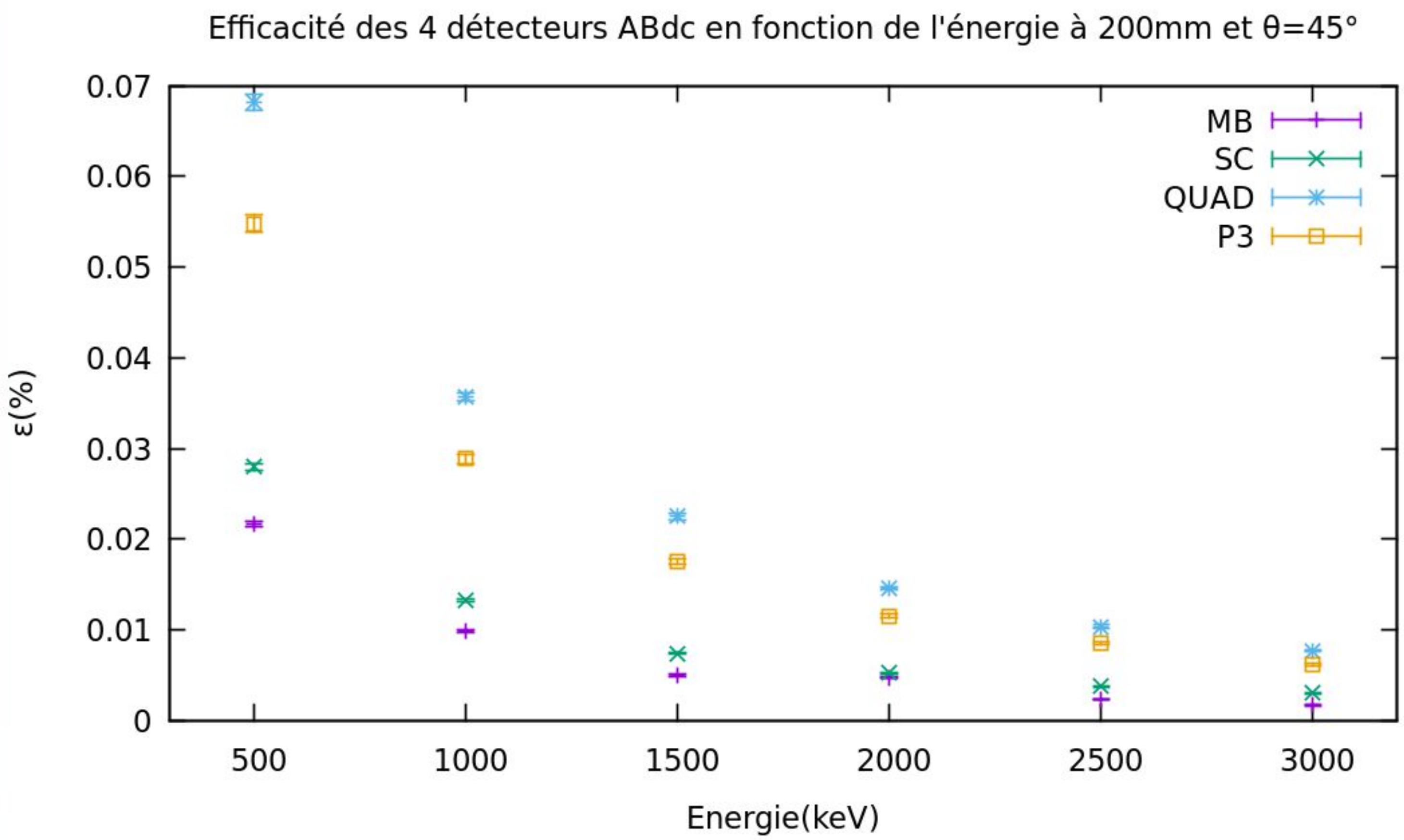
Efficacité des 4 détecteurs ABdc en fonction de l'énergie à 200mm et θ=45°
ε(%)
0.07
0.06
0.05
0.04
0.03
0.02
0.01
0
500
1000
1500
2000
2500
3000
Energie(keV)
MB
SC
QUAD
P3